

Local structural investigation of Zr & Ca doped BaTiO₃ nanocrystals

Thesis submitted for fulfillment of the requirements for the degree of

Master of Technology in

Nano Science & Technology

Jadavpur University

Submitted by

AMIT MAITY

Exam roll no: M4NST22017

Registration no: 154586 of 2020-21

Under the joint guidance of

Dr. Jiten Ghosh

Principal Scientist

Material Characterization Division

CSIR- Central Glass and Ceramic
Research Institute,

Kolkata-700032

Dr. Chandan Kumar Ghosh

Assistant Professor

School of Materials Science and
Nanotechnology

Jadavpur University

Kolkata - 700032

August, 2022

CERTIFICATE OF RECOMMENDATION

This is to certify that the thesis entitled “Local structural investigation of Zr & Ca doped BaTiO₃ nano-crystals” is done by AMIT MAITY under the supervision and guidance for partial fulfillment of the requirement of master of Technology in nano Science and Technology in School of Materials Science and nanotechnology, Jadavpur University during the academic session 2020-2022.

Dr. Jiten Ghosh

Principal Scientist

Material Characterization Division
CSIR-CGCRI, Kolkata

(Guide)

Dr. Chandan Kumar Ghosh

Assistant Professor

School of Material Science and
Nanotechnology,
Jadavpur University

(Co-guide)

DEAN

Faculty Council of interdisciplinary Studies Law and Management
Jadavpur University,
Kolkata -700032

Certificate of approval

The thesis is hereby approved as a credible study of an engineering subject carried out and represented in a satisfactory manner to warrant its acceptance as a prerequisite to the degree for which it has been submitted.

It is to be understood that by this approval the undersigned does not necessarily endorse or approved any statement made opinion expressed or conclusion drawn there in but approved the thesis only for the purpose for which it has been submitted.

Signature of the Examiner

.....

.....

.....

.....

**DECLARATION OF ORIGINALITY AND COMPLIANCE OF
ACADEMIC ETHICS**

I hereby declare that, this literature contains survey and original research work by the undersigned candidate as part of Master of Technology (Nano-science and Technology) studies during academic session 2020-2022.

All the given information in this document has been obtained and presented in accordance with academic rules and ethical conduct.

I also declare that, as require by this rules and conduct, I've completely cited and referred all information and results are original to this work.

Name : AMIT MAITY

Roll no : M4NST22017

Thesis Title : Local structural investigation of Zr & Ca doped BaTiO₃
Nano-crystals

Signature with Date:

ACKNOWLEDGEMENT

While bringing out this thesis paper to its final form, i came across a many people whose contributions in various ways helped me to understand my field of knowledge and research and they deserve special thanks for that. It is a pleasure to convey my gratefulness to all of them.

I would like to express my sincere and heartfelt gratefulness to my guides Dr. Jiten Ghosh (CSIR-CGCRI) & Co-guide Dr. Chandan Kumar Ghosh (Jadavpur University) for sharing their knowledge with me, guiding me in my work at CSIR CGCRI & Jadavpur University. The ideas and guidance they have provided me are invaluable. Their motivation has helped me to finish my thesis work in proper way.

I also express sincere gratitude to Dr. Suman Kumari Mishra, Director, CSIR-CGCRI, Kolkata for provide me with an opportunity to undergo my M. Tech project at CSIR-CGCRI, Kolkata. I am also thankful to Dr.Tarun Kumar Kayal (chief scientist & head MCD), for giving this opportunity to work in the Material Characterization Division of CSIR-CGCRI.

I would like to thank Dr. Jiten Ghosh for his assistance to carry out different experiments at MCD division. I would like to thank Dr. Santanu Sen, Mr. Nirmal Ghosh, Mr. Prosenjit Khan, Mr. SumitNath, Sahnoor Islam, Kanchan Kole and Asish Jana for their never-ending support and for keeping such memorable assessment. I would like to thanks all the staff members of Material Characterization Group. I would like to thanks each and everyone else who helped me in the completion of my project.

I am also grateful to all my classmates, who always gave me a constant co-operation and support throughout the project work. I am also thankful to all the stuff members of the department for their full co-operation and much needed help.

My greatest thanks are to all who wished us success especially my parents and friends whose support and care make our stay on Earth.

*Dedicated to My Parents, My Guides &
My little Sister*

Table of Contents

Page no.

| | |
|----------------------|-------|
| List of Figures..... | (i) |
| List of Tables | (ii) |
| Abstract..... | (iii) |

Chapter 1: introduction

| | |
|---|----|
| 1.1 introduction to nanoscience & nanotechnology..... | 2 |
| 1.2 What is nanotechnology..... | 2 |
| 1.3 How it started.. .. | 2 |
| 1.4 Who come the term nanotechnology?..... | 3 |
| 1.4.1 A brief history of nano-technology:..... | 3 |
| 1.5 What distinguishes nanomaterial from bulk?..... | 4 |
| 1.6 The use of nanomaterial provides following advantages | 4 |
| 1.7 Classification of nano-materials:..... | 7 |
| 1.8 Synthesis of nanomaterials:..... | 7 |
| (1) Top Down and Bottom Up approach..... | 9 |
| (2) According to growth phase approach:..... | 10 |
| (3) According to the form of products approach:..... | 10 |
| (4) Self-assembly:..... | 10 |
| 1.9 applications of nanotechnology..... | 10 |
| a) Nanotechnology in Energy and Environment:..... | 12 |
| b) Nanotechnology in Flexible Electronics:..... | 12 |
| c) Nanotechnology in Health and Medicine:..... | 13 |
| d) Nanotechnology in Transportation:..... | 14 |
| e) Nanotechnology in Defence and Security:..... | 14 |
| f) Nanotechnology in information & Communication:..... | 14 |
| 1.10 Theory of Pair distribution function (PDF) PDF:..... | 15 |
| 10.1 Information about PDF;..... | 15 |
| 10.2 Application of PDF in nanomaterials-..... | 16 |
| 1.11 Future transport benefits..... | 16 |

| | |
|---|----|
| 1.12 Types of nanoparticles..... | 17 |
| 1.12.1 Three-dimensional nanomaterials (3-D)..... | 19 |
| 1.12.2 Two-dimensional nanomaterials (2-D)..... | 19 |
| 1.12.3 One-dimensional nanomaterials (1-D)..... | 19 |
| 1.12.4 Zero-dimensional nanomaterials (0-D)..... | 20 |
| Reference..... | 21 |

Chapter 2: General Overview on BaTiO₃

| | |
|--|----|
| 2.1 Introduction of BaTiO ₃ | 24 |
| 2.2 Crystal Structure, nono- stoichiometric and Defect Chemistry of BaTiO ₃ | 25 |
| 2.3 introduction BCZT :..... | 25 |
| 2.4 Dielectric Properties:..... | 26 |
| 2.5 Purpose of Doping..... | 26 |
| Reference..... | 28 |

Chapter 3: Literature review 30

| | |
|----------------|----|
| Reference..... | 33 |
|----------------|----|

Chapter 4: Experiment

| | |
|--|----|
| 4.1 Experimental Set up:..... | 35 |
| 4.2 Material Synthesis..... | 35 |
| 4.2.1 Fritsch ball milling: -..... | 35 |
| 4.2.2 Furnace..... | 36 |
| 4.2.3 Sonicationbath..... | 36 |
| 4.3 Materials Characterization tools | 37 |
| 4.3.1 X-Ray diffractometer (XRD)..... | 37 |
| 4.3.2 FESEM (Field-emission Scanning Electron Microscope)..... | 38 |
| 1. Principle..... | 38 |
| 2. Preparation | 39 |
| 3. Source of electrons | 39 |
| 4. image formation..... | 39 |

| | |
|--|-----------|
| 5. Working principle..... | 40 |
| 4.3.3 Fourier Transform Infrared Spectroscopy (FTIR):..... | 41 |
| i) Principle of operation..... | 41 |
| 4.3.4 Pair Distribution Function (PDF) | 42 |
| 4.3.5 Di-electric Measurement..... | 43 |
| 4.3.6 TGA and DTA –..... | 44 |
| 4.4 Experimental procedure:..... | 45 |
| Chapter 5: result and Discussion | |
| 5.1 XRD analysis of BCZT powder-..... | 47 |
| 5.1.1 Characterization BCZT-1..... | 47 |
| 5.1.2 Characterization BCZT-2..... | 50 |
| 5.2 PDF analysis..... | 53 |
| 5.3 FESEM analysis..... | 54 |
| 5.4 FTIR (Fourier Transform Infrared Spectroscopy)..... | 57 |
| 5.5 TGA _ DTA analysis..... | 57 |
| 5.6 Dielectric constant | 58 |
| Chapter 6: Conclusion and future Scope | |
| Conclusion..... | 61 |
| Publication..... | 62 |
| Reference..... | 63 |

List of Figure

page no

| | |
|--|----|
| Fig.1.1: surface/volume ratio as a function of particle size | 5 |
| Fig.1.2: schematic diagram of different synthesis approaches of nanomaterial | 8 |
| Fig.1.3: Schematic diagram of top down and bottom up approach | 9 |
| Fig.1.4: applications of nanotechnology | 11 |
| Fig.1.5: (a) Schematic illustration of generation of pair neighbors the origin atom and (b) corresponding peaks in radial distribution function. | 15 |
| Fig.1.6: Classifications of nanoparticles according to their morphology, Composition and dimensionality. | 17 |
| Fig.1.7: classification of nanomaterials. | 19 |
| Fig.2.1: Unit cell of BaTiO ₃ | 25 |
| Fig.3.1:- Planetary Ball Milling (Fritsch) | 35 |
| Fig.3.2:- Sonication bath | 36 |
| Fig.3.3- X-Ray Diffractometer (Rigaku Ultima-iii) | 37 |
| Fig.3.4:- Field-Emission Scanning Electron Microscope (FESEM, sigma, Zeiss) | 40 |
| Fig.3.5:- Schematic diagram of the FTIR spectrometer | 42 |
| Fig.3.6: – Bruker D8 advance | 43 |
| Fig.3.7:- Dielectric measurement instrument (Wayne kerr 6500B) | 44 |
| Fig.5.1:- XRD pattern of starting and milled (0-100 h) BCZT-1 sample | 49 |
| Fig.5.2:- Comparison of all XRD pattern at starting and milled (0-100 h) BCZT-2 sample | 49 |
| Fig.5.3:- Rietveld refinement of BCZT-2 (100 hrs) | 51 |
| Fig.5.4:- XRD pattern of starting and milled (0-100 h) BCZT-2 sample | 52 |
| Fig.5.5:- Comparison of all XRD pattern at starting and milled (0-100 h) BCZT-2 sample | 52 |
| Fig.5.6:- Different bond distance and atomic arrangements of BaTiO ₃ obtained from PDF | 53 |
| Fig.5.7: FESEM image of BCZT-1 and BCZT-2 (1 to 6) | 55 |

| | |
|---|----|
| Fig 5.8: Particle size variation with milling hrs (a) BCZT-1 and (b) BCZT-2 obtain from FESEM | 56 |
| Fig.5.9: EDX spectra BCZT ceramic sample | 56 |
| Fig.5.10:- FTIR spectra of heat treated powder at different ball milling time. | 57 |
| Fig.5.11:- DTA-TGA curves obtain from BCZT powder | 58 |
| Fig.5.12: Dielectric value of BCZT-1, BCZT-2 and Pure BT sample. | 59 |

List of Table

| | |
|---|----|
| Table 1.1: Categories of nano materials | 7 |
| Table.2.1. The important properties of BaTiO ₃ | 24 |
| Table.5.1: Wt. % of phases, values of Unit cell parametets and Unit Cell volume as obtained by Rietvled Analysis for BCZT-1. | 47 |
| Table.5.2: Value of crystalline size and lattice strain of Ba _{0.85} Ca _{0.15} Zr _{0.04} Ti _{0.96} O ₃ (BCZT-1) | 48 |
| Table.5.3: Wt. % of phases, values of Unit cell parametets and Unit Cell volume as obtained by Rietvled Analysis in BCZT-2. | 50 |
| Table.5.4: Value of crystalline size and lattice strain of Ba _{0.85} Ca _{0.15} Zr _{0.10} Ti _{0.90} O ₃ (BCZT-2) | 53 |
| Table.5.5:- comparison of different bond distance and atomic arrangements of BaTiO ₃ obtained from PDF | 54 |
| Table.5.6: Dielectric and capacitance in different milling time variation | 59 |

Abstract:

Barium titanate ceramic is one of the technologically important lead free materials for piezoelectric and tunable capacitor device applications. The technological trend towards decreasing dimension makes it of interest to examine its functional properties at nano-scale due to the miniaturization of electronics devices. In the present work, lead free BCZT ceramics i.e $\text{Ba}_{0.85}\text{Ca}_{0.15}\text{Ti}_{0.96}\text{Zr}_{0.04}\text{O}_3$ and $\text{Ba}_{0.85}\text{Ca}_{0.15}\text{Zr}_{0.10}\text{Ti}_{0.90}\text{O}_3$ has been prepared by high energy ball milling to study the local distortion in lattice due to presence of dopants (Zr, Ca etc) and its effects on the formation of polar nano regions (PNR's) in nano-structured Ba-based perovskite. XRD, PDF, FESEM, FTIR, TG-DTA are used to structural characterization of BCZT. The dielectric property depends on this local atomic arrangement of Zr and Ca atoms in BaTiO_3 and coexistence of multiple phases. The knowledge of such understanding will lead to the synthesis of lead free BCZT ceramics. The short range and long range structure reported from PDF curve fitting with local and average structure investigate. Very small amount of dopant (Zr, Ca) can considerably modify functional properties like the electrical conductivity and the domain wall mobility. The phase transformation behavior of BCZT powder will be studied with particle size reduction and finally dielectric properties will be correlated with the structure at nano-scale.

Keyword: Lead free BaTiO_3 , BCZT, XRD, PDF, Local Structure, High energy ball milling, Di-electric Constant, TGA-DTA.

Chapter 1: Introduction

1.1 Introduction to Nano-science & Nanotechnology:

Nano technology deals with materials, engineering, and technology conducted at the nanoscale, which is about 1 to 100 nanometers. One nanometer is a billionth of a meter, or 10^{-9} of a meter. Nanotechnology is defined by size naturally very broad, including the field of science and technology as surface science, organic chemistry, molecular biology, semiconductor physics, energy storage capacitance, microfabrication, molecular engineering, etc. nanotechnology is manipulating the matter on an atomic, molecular, and super molecular scale. The associated research and development are equally diverse, ranging from extensions of conventional device physics to completely new approaches based upon molecular self-assembly, from developing new materials with nano-dimensions on the nanoscale to direct control of matter on the atomic scale.

1.2 What is nanotechnology?

Most study revolves around the control of phenomena and materials at length and size scales below 100 nm and quite often they compare with a human hair, which is about 80,000 nm. It is seen that a size range to the 1-100 nm, the area where size-dependent quantum effects come to bear, would exclude materials and devices, especially in the pharmaceutical area, and some experts take issue against a rigid definition based on a sub-100 nm size. This study reflects the fact that quantum mechanical effects are important at this quantum-realm, and so the definition shifted from a particular technological to a goal for a research category work, inclusive of all types of research and technologies which deal with the special properties of matter which occur below the given size threshold. It is therefore common to see the plural form "nanotechnologies" as well as "nanoscale technologies" to refer to the broad range of applications and research whose common trait is size.

Another important point for the definition is the requirement that the nano-structure is manmade, synthetically making nanoparticle or nanomaterial. Otherwise we would like have to include every naturally formed material and bio-molecular particle, in effect redefining much of chemistry and molecular biology as 'nanotechnology'.

1.3 How it started?

The concept and ideas behind the nano science and nanotechnology started with a talk entitled 'There's plenty in a Room at the Bottom' by physicist Richard Feynman at an American Physical Society meeting at the California Institute of Technology on December 29, 1959; a long time before the term nanotechnology was used. In this talk, Feynman described a process in which scientists would try to manipulate and control molecules and atoms. Therefore, physicist Richard Feynman is known as father of nano-technology.

1.5 Who come the term nanotechnology?

The term nanotechnology comes in 1974 by Norio Taniguchi of Tokyo science University to describe the processes semiconductor processing such as thin film deposition which deals with control on the order of nanometer. It wasn't until 1981 with development of the scanning tunneling microscope (STM) it could see individual atoms with modern nanotechnology began. He inspired by Feynman's concept, in 1986 K. Eric use "nanotechnology" term in his book Engineering of creation. Upcoming era of nano technology the idea of a nanoscale "assembler" proposed. In which be able to build a copy of itself and of other things are arbitrary complexity with atomic control.

Now a days engineers and scientists are finding a wide range of advantage to deliberately make new material at the nanoscale, and enhanced the properties like higher strength, light in weight, increase control of light spectrum, and high chemical reactivity than their large scale or bulk quantity.

1.4.1 A brief history of nano-technology:

Before 2000 years: Romans and Greeks are use sulphide nano crystal on their hair for dye

Before 1000 years ago: Gold Nanoparticles use in different sizes for making colors stained glass and window.

In 1959 physicist Richard Feynman was give a lecture on an American physical lab. Title name "there's plenty at room the bottom".

1974 professor norio Taniguchi first time used the name nanotechnology

1981: IBM invented scanning tunneling microscope.

1985 scientists at Rice University and University of successfully discover Fullerene also called "Buckyball".

In 1986 First book on nanotechnology is "Engineering of Creation" by K. Eric Drexler.

1986 Atomic Binnig, Quate and Gerbe are invented atomic force microscope.

1989: IBM invented logo using atoms.

1991: S. Ijima discovered carbon monotubes

1999 R. Freitas write firtnano medicine book name by "Nano medicine".

2000: national nanotechnology was initiative launched.

2000-2021: various type of innovation involves in last 20 years like, nature of carbon fiber, drug delivery, advances of transparent conductive thin films, frontier for droplets in droplets,

world's smallest hacky sacks, spray drying technique for making noise in gene silencing. Electric vehicle charging, fire proof nanomaterial bringing etc [1].

1.5 What distinguishes nanomaterial from bulk?

Most of nano structured material have their same material properties to the corresponding bulk material, nanometer have their material and dimension properties which are significantly different phase those of atoms and bulk material. The characteristics of nanomaterial that difference from bulk materials. The following characteristic are.

- A) High surface of fraction.
- B) Large surface energy.
- C) Spatial confinement.
- D) Decrease number of imperfections that can't exist in the corresponding bulk material.

1.6. The use of nanomaterials provides following advantages:-

First of all, nanomaterial contains of very small particles. This is the most advance of nanomaterial properties who promoting attained of super miniaturization. Because they are in small size, nano structured can be bonds very tightly each other. As a result, it's give a unique area one can located more advice functional nano device. Which is high effectiveness output device in nano electronics. The high packing density has potential to bring large specific area and high volume information capacity storage and high speed information processing device (because free electrons take much less time for travel one atom to other atom between components). Thus new concert arrived for making electronic devices which is smaller and faster circuit more sophisticated function and greatly minimize powder consumption that can all achieve simultaneously by controlling interaction nano structured and complexity structure.

Secondly, because of their small size in dimension, nano-material have more specific surface area, which accelerating interaction between them and they located in the environment. Nano particle have much higher surface area per unit mass as compared with the large particles size. Therefore, growth and catalytic chemical reaction occur at surface of material. This means that materials in nano parties will be much higher reactive than same mass of nanomaterial with built in large particle. The high increase in the participation of surface/face atoms in physically and chemically properties of nanomaterial is another consequences of decrease in particle size. It's know that 3^{rd} power decrease it's linear dimension of an object and decrease in 2^{nd} power in specific surface area in case of nanoparticles. The surface ratio in area to volume increase than nominal size [2]. The variation of surface to volume ratio as a function particle size is given in Fig. The surface atom of a nano particles have unusual parameters that surface atoms make Nanoparticles very close packed particle, because the bonds are not attached surface atoms with neighboring atoms are enabled. For atoms on uneven surface no saturation of the highest bonds. For this reason, corner atoms

normally have highest affinity to from bonds who absorbed molecules for the catalytic activities followed by edge and in plane surface atoms as a face that is of great importance. Alternatively, in thermodynamics equilibrium the low stabilization due to low coordination in edge and particular corner atoms are often missing single crystal. Recently cerium oxide nano particles are size dependent variation in oxidation phase and lattice parameter has been reported.

As a result of the changes that occur in particles with a reduces of particle size, nanomaterials can have extremely high biological and chemical reactivity. For example, catalytically active nanomaterials allow increase either physical or chemical or biochemical reactions by tens of thousands, and even a million times. This attribute explains even 1 g of nano-material can be more effective than 1 ton of a similar but macro particle.

Another aspect we must consider that the free surface is a place where accumulation of crystallographic defects shown. At small particles sizes, the surface concentration of defects increases considerably. Hardeveldand Hartogin 1969 estimated the largest change in proportions between face, edges and corner micro defects occurred at the surface between 1 and 5 nm [11].As a result, lattice distortion and even a small change of lattice type that can take place on the surface layer. In fact, due to accumulation of structural defects and chemical impurities on the top plane, we can seen purification of the bulk area of the nano-particles. Properties of nano materials change with its dimension [8]. Recently researchers are involved to study the unique properties at nano scale which are not conventionally showed at the bulk materials.

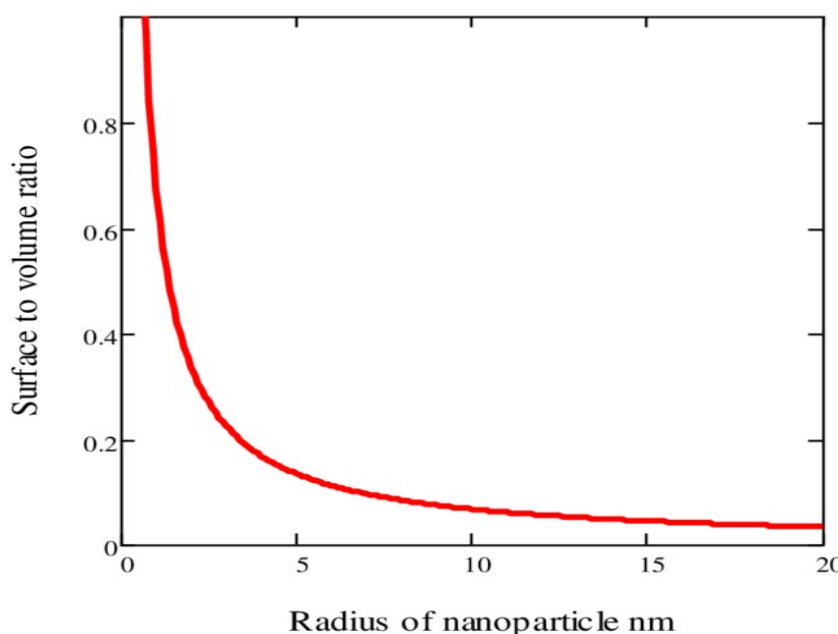


Fig.1.1: surface/volume ratio as a function of particle size

An important specific characteristic of nano-material properties (we mean here polycrystalline materials with grains size less than 40 nm) is an increase of the role of interfaces with reduce of the size of grains or crystallites innano-materials. Experimental research has shown that the state of grain boundaries has an in equal character, conditioned by the presence of the highest concentration of grain boundaries defects. This non-equilibrium is characterized have extra energy of the grain boundaries and by the presence of long-range elastic stress. At the same time, the grains have ordered crystallographic structure, while the grain boundary defects produce as a source of elastic strains. non-equilibrium of the grain boundaries initiates the maker of the lattice distortion, the change of intra-atomic distances, and the appearance of sufficient spacing of atoms, right up to loss of an ordered state.

Another important factor peculiar to nano-particles is their probability to aggregation. The possibility of migration (diffusion) of either atoms or groups of atoms along the surface and the boundaries, as well as the presence of attractive forces between atom, often leads to processes of self-organization into various nano structures. This effect has been used for creation of ordered nanostructures in optics and electronics device.

One more important point of nanomaterial properties is connected with the fact that, during transport processes (diffusion, electro- and thermal conductivity, etc.), there are certain effective lengths of free path of a carrier of this transport, such as election and phonon which is free mean path, the Debye length and the diffusion election length for certain polymers. While proceeding to smaller size than transport speed starts to depend on both the size and the shape of the nanomaterials; basically, the transport speed increases with sharply [12].

The principal characteristics of nanomaterials are conditioned by not only by their small the size, but also by the appearance of new quantum mechanical effects ina dominating role at the interface (Esaki 1991 [13]; Serenaand Garcia 1997 [14]). Those quantum size effects occur at a critical size, which is proportionate with the so-called correlative radius of one or another physical phenomenon, in example, with the length of the free path of electrons or photons, the length of coherence ina superconductor, sizes of magnetic domains, and so on.

As a point, quantum size effects shown in materials with crystallite sizes in the nano-range $d < 10$ nm. As a result, In nano materials with characteristic size and shape, one can expect the appearance of effects which cannot be observed in bulk materials.

1.7 Classification of nano-materials:

Nano-materials can be Classified dimension wise into following categories shown in Table 1.1[1].

On the basic composition phase nanomaterial in different phases can be classified as [3],

- In single phase solids have amorphous crystalline and layer materials etc
- In multiphase solid particular include composite matrix coated particle etc [4].
- In multiple phase system make collides Ferro fluids and aerogels are present.

Table 1.1: Categories of Nano materials

| <i>Classification</i> | <i>Examples</i> |
|-----------------------|------------------------------|
| Zero dimension<100nm | Dots, hollow spheres, etc |
| One dimension<100nm | nanorods, nanowires, etc |
| Two dimension<100nm | Tubes fibers, platelets, etc |

1.8 Synthesis of nanomaterials:

In order to explore the unique physical properties & phenomena and it also to Realise the useful application of nano material and nano structure that ability to fabricate and process material and nanostructures in the first hurdle in nanotechnology. The following schematic diagram in Fig. 1.2 shows the two significant approaches in the synthesis of nanomaterial [26,5].

Some challenges take place for the care of the fabrication and processing of nano materials and nanostructure.

1. To overcome the large surface energy, as a result of enormous surface area or higher surface to volume ratio. Large surface area with high surface to volume ratio [8].

2. It ensures that all nanomaterial with help desire size and uniform distribution size morphology crystallinity and chemical composition and microstructure which result in describe physical properties. Uniform particle size with uniform partials morphology.
3. Prevention of nanomaterial and nano structure form coarsening through either overlapping or agglomeration of nano materials.

Many of technologies that had been explored on fabricate nano structure and nano material. This technical approach can be assembled in several way like growth media or the form of product [6].

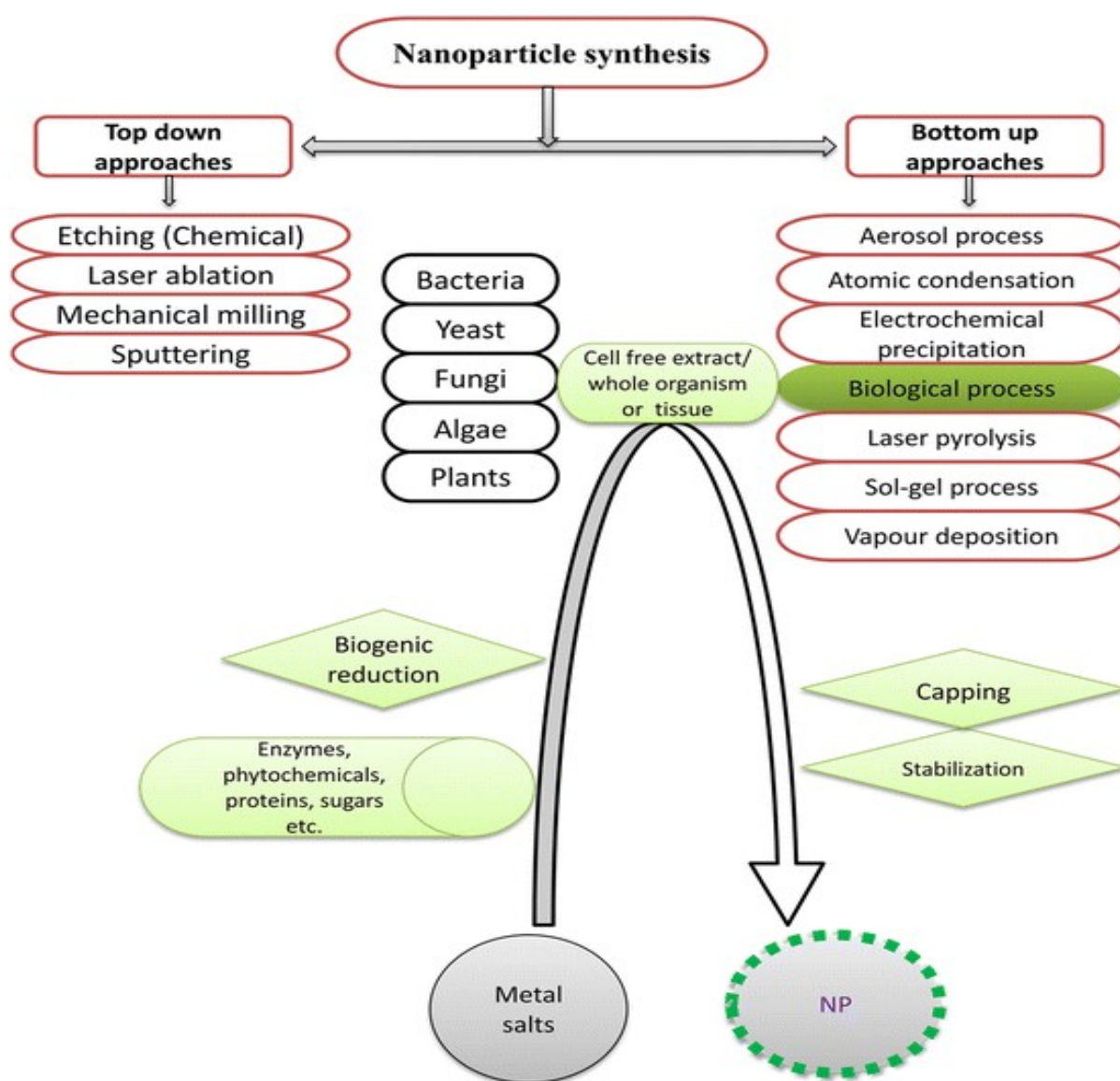


Fig.1.2: schematic diagram of different synthesis approaches of nanomaterial

(5) Top Down and Bottom Up approach

The common method used to guide the synthesis of nanoscale material is the top down approach. The proper diagram is defining in generally detects that in the top down approach it's being from a ball size of material which is gradually or step by step remove from an object in the nanometer scale. This technique is known as search photo lithography and Electron beam lithography [7], Ionization and plasma itching all belongs to this type of approach. The top down approach is exactly opposite to the bottom up approach.

In this case instead of using large material and chipping its way to break into small bites, all I start from atoms and molecules that gate arranged and assemble to a large nanostructure. The synthesis of a new particles in the nanotechnology world as the bottom approach is to allow making a diverse type of material [9]. It is likely to revolutionize the various way of material synthesis and fabrication. Symmetric representation of bottom up and top down approach is shown in figure. Meaning is a common approach for top down method to making nanoparticle, where is the colloidal dispersion is a good example of bottom up approach in the nanoparticle synthesis.

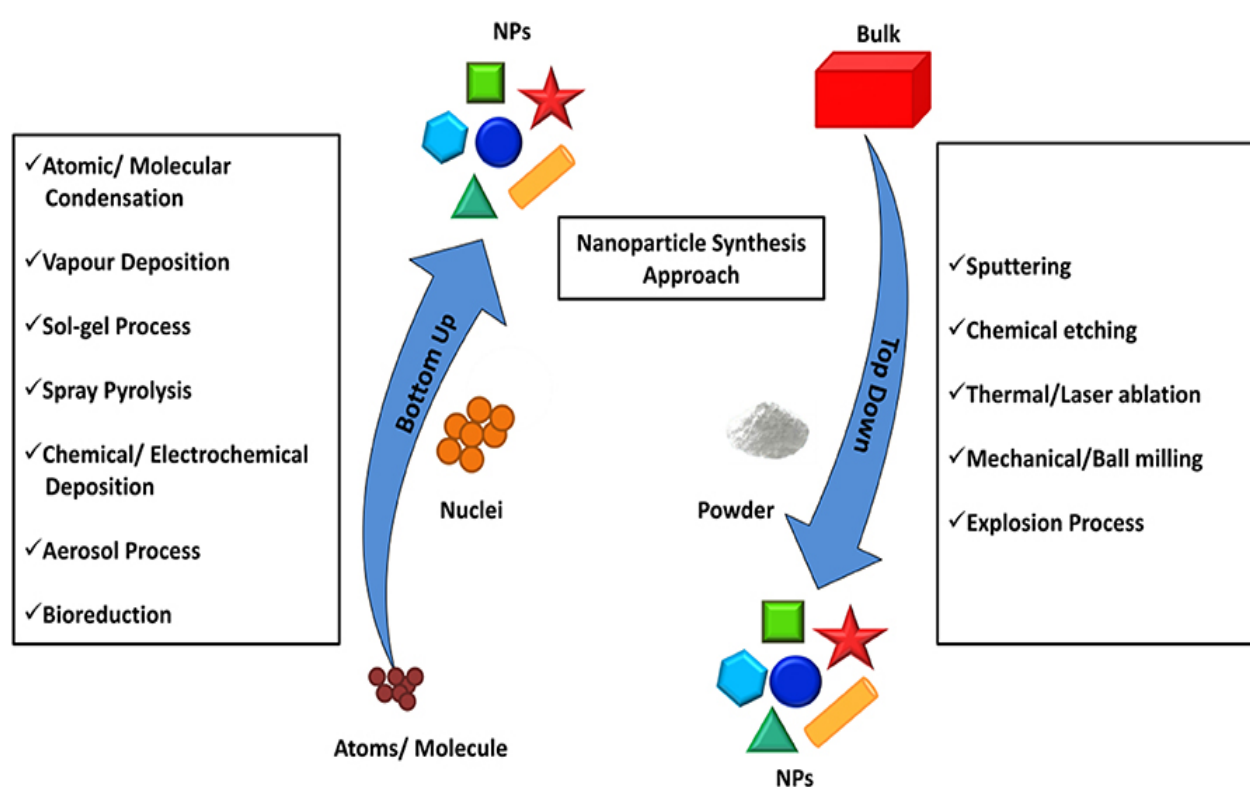


Fig.1.3: Schematic diagram of top down and bottom up approach.

(2) According to growth phase approach:

(a) In vapours phase introduce the growth of laser reaction pyrolysis for nanoparticle synthesis and atomic layer deposition for making the thin film deposition.

(b) In liquid phase growth collide particle including nanoparticles our formation of self-assembly to nanolayers.

(c) In solid phase formation the phase including to segregate metallic particle to make a glass unit.

(3) According to the form of products approach:

(a) In colloidal Processing the nanoparticle flames combustion and phase segregation.

(b) Nano rods and nano wires use by for making template based electroplating, solid liquid solution and spontaneous anisotropic growth.

(c) Molecular beam epitaxial an atomic layer deposition is used for making thin film.

(4) Self-assembly:

Once bottom up approach is natural path self-assembly is introduce. the self-organizing process are common throughout the making a new compounds from the molecule To the small scale and even beyond. Ducky using for self-assembly as a controlled and directed fabrication process lies in between designing the component data required to self-assembly into a desire pattern and functions. In self-assembly process material collect the information code like shape, size, surface properties, polarizability, mass, change magnetic dipole etc. In individual compounds that are determine by the Characteristic of the material are connect among them.

1.9 applications of nanotechnology

Nano technological application is execute in different field of research with the various unique field of applications. When a particle is break to nano-scale, several properties changes of the material accordance with size. So it gives new thought of applications in several fields. Therefore surface to volume ratio increases, so it gives more surface area to react. Several optical as well as mechanical properties are also dependent on the diameter or the size of particles [10].

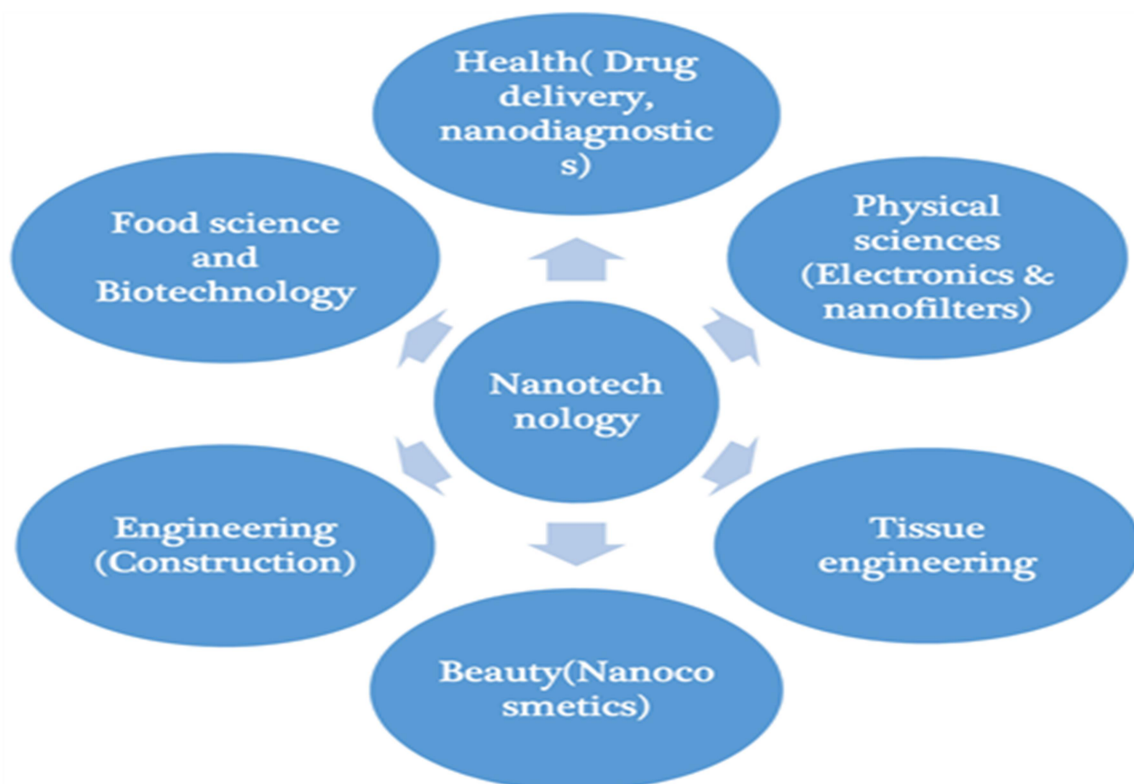


Fig.1.4: applications of nanotechnology

nanotechnology has innumerable applications in variety of diverse fields all of which are interconnected with each other. The modern world has burgeoned in a consequential extent with the advent of newer technologies based on nano science [17]. The applications include nanoscale patterning of electronic circuits, high density data storage, quantum computers, fuel cell catalysts, industrial catalysts, environmental catalysts, waste water treatment, functional nano-composites, food packaging, food processing catalysts, hydrogen production in photocatalysts, automotive catalysts, fuel additive catalysts, Lithium ion battery, electrodes, reinforced plastics, natural or synthetic polymer hybrid fibers, controlled drug release, cancer therapy, drug delivery, bio imaging, bio markers [13], hyperthermia treatment, MRI contrast agents, infra ray contrast agents, ultra violet protection like sunscreens, antioxidants, ultra violet blocking coatings, water resistant coatings, gas barrier coatings, anti-microbial coatings, self-cleaning building surface, food quality and safety analysis sensors, chemical sensors, gas sensors, high sensitive sensors, pollution monitoring sensors, functional nanocomposites, nano pigments, super thermal-conductive liquid, nano phosphors for display, super plastic ceramics, transparent conductive polymer films [25], chemical mechanical planarization, nano inks, single electron transistors, quantum lasers, high power magnets, pollutant scavengers, interactive food, nutraceutical, fungicides and pesticides, medical textiles, technical textiles, heat retaining textiles, self-cleaning textiles, anti-stain textiles, electro-conducting textiles, ultra violet blocking textiles, wound dressing, dental

ceramics, bone growth, tissue cells engineering, molecular tagging, solar cells dye sensitized, paint-on solar cells, hydrogen storage materials, bio-composites, Ferro-fluids, refractive index engineering, aerospace engineering and many others.

Detail applications in some important fields are given below:

(a). Nanotechnology in Energy and Environment:

Energy crisis and environmental pollution in present days have severe negative impact in human life. To provide sufficient energy to the developing world, nanotechnology is the key factor because less expensive improved energy can be produced through suitable nanomaterial. Recent nanotechnology projects to diminish the energy crisis is related to the parameters like storage, conversion, sufficient super capacitance and recyclability production with the help of small amount of nanomaterial, thermal insulation increment etc. Energy application with the help of nanomaterial:

- (1) Fuel cell (e.g. CNT) for hydrogen storage and related automobile applications.
- (2) Cheap, light weight and high efficient metal oxide nanomaterial photovoltaic application for the purpose of water splitting and efficient dye sensitized solar cell.
- (3) Nanotechnology that can used to further reduction of pollutant from combustion engine by making nanoporous filter, which can replace the mechanical exhaust.
- (4) nanotechnology in water disinfection with the help of nanostructured photosensitized catalyst and further step towards environmental safe and green technologies.
- (5) Solid state lighting is a powerful tool to decrease the total electric consumption by 10% and eliminate carbon emission into the environment by equivalent of 29 million tons per year.

(b). Nanotechnology in Flexible Electronics:

Nanotechnology in electronic industry is gradually becoming popular because smaller size and compact design of electronic devices can ensure faster processing, reduction of delay in circuitry and processing power consumption. Nanotechnology in electronics industry introduces microprocessors less than 100 nanometers (nm) in size. However, nanoelectronics are basically the extension of microelectronics and research in nano electronics will develop CNT, Graphene based flexible independent electronic devices in future.

- (1) Carbon Nano Tube (CNT) based field emission display is highly efficient because light weight CNT can be used as a field emitter with high efficiency up to 90% and field emission display have low power consumption.

- (2) The nanotechnology is use in memory card to increase the density. In research and development, a memory chief with the high density of one terabyte of memory per square inch or less. Integrated Nano sensor is used for processing and communicating massive amount of data into a minimum size and weight with low power consumption.
- (3) Research in nanotechnology introduces transistors with Graphene and CNT as active materials and CNT transistor based processor for computer application is about to commercialize in future market. Due to their small size and power consumption is low; CNT and Graphene based transistors are easy to integrate in the integrated circuits.
- (4) Large magnetic moment and adequate coercively nanomaterial can help to produce magneto caloric effect on a particular scale so that refrigeration could be possible without need of refrigeration fluids.

(c). Nanotechnology in Health and Medicine:

Nanotechnology has a high impact on the research and applications related to biology and medicine. Nano-drug delivery [15] is the safest procedure for medication because small quantity of nanomaterial can help to recover with reducing side effects. Nano medicine has also the big potential in medical field to enable early detection and prevention, and with the help of biosensor to ensure the high quality treatment provided for diagnosis treatment and disease in medical field.

- a. Carbon Nano Tubes (CNT) have promising application for developing of advance biosensor with the new features.
- b. CNT, can be functionalized at the tip with a probe molecule. CNT [16,18] can be used in the following areas of nanao technology.
 - i. Leukaemia cells identification
 - ii. Catheter development.
- c. Nano devices can make gene sequencing high efficient.
- d. Tissue engineering that makes use of artificially stimulated cell which can help in transplantation of organs or artificial implants.
- e. This type of technology is also use to develop a sensor for the cancer patient for diagnosis [14].

(d). Nanotechnology in Transportation:

Nano material's used as faster and cost effective new fuel source. The main advantage of caring nano-materials light weight so that easy to carry in fuel chamber of cars and aero planes.

(1) Suitable nano materials can effectively reduce the emission of pollutants in the process of incomplete combustion in engine. nano Twin Technologies has recently released an air filter to eliminate hazardous chemicals from the air in car cabins.

(2) Nanoparticles of inorganic clays and polymers are an effective alternative for carbon black tires results in environmental friendly, wear resistant tires. Frictional resistant tires are also made possible through nano science.

(3) Nano coating on metallic surfaces such as steel to get super-hardening, low friction, and increase corrosion protection.

(e) Nanotechnology in Defense and Security:

Nanotechnology can used to give protection, more lethality, longer endurance and better self protection capacity of future combat soldiers. The advantages are expected to great by which include thread detection, Nobel electronics display and interface system, as well as provide a roll for the development of a arm combat vehicle and robotics. This technology can use for night vision camera also. The nano technology will also a tiny portable sensor system who capable of identify biological and chemical weapons as, and can protect from nuclear and radiation threats.

(f) Nanotechnology in information & Communication:

In the past the electronic memory design on the formation of transistor. For research and development in electronics industry to reduce the driving force depends on nano science and technology. According to sorting silicon chip is getting expensive and difficult for making. This century chip industry is use to build the molecule transistors, the industry's focus on for building faster cheaper chips. Philip Kuckes says that "With the electronics we are talking about, we are going to make a faster computer that does not just fit in your wrist watch, not just in a bottom on your shirt, but one of the fiber of your shirt". According to the making nanotube base nonvolatile random access memory is a universal memory chip suitable for countless existing and new application in the electronics field. Quantum dot laser are cheaper than conventional laser which is offer a high beam quality then conventional diode laser. In the modern technology traditional communication analogue circuit device are rapidly replaced by optical or optoelectronics device due to their high bandwidth and capacity. They are to promising examples are photonic crystals and quantum dots. Quantum dots are objects

in nanoscale, which can use for laser construction. The main advantages of a quantum dot laser over the traditional semiconductor they are emitted wavelength depend on the diameter of the dot.

1.10 Theory of Pair distribution function PDF:

The shape convolution method is used to calculate the diffraction pattern of the disordered or nanomaterials based Debye scattering function followed by the pair distribution function (PDF) analysis. The atomic pair distribution function is defined as the probability of finding any two atoms which are separated by distance " r ". The function will produce a peak which is finding an atoms with respect to another atom corresponding to the inter-atomic distance r [19]. In geometrical point of view the atomic PDF is a function gives the probability of finding atoms in a spherical shell of unit thickness at a radial distance r from reference distance atom. Peak position in a PDF gives the characteristic distance of separating pairs of atoms reflect the local structure of materials [20].

10.1 Information about PDF;

In PDF graph three type of information get-

- Peak position*- The peak position corresponding to quantitative atomic distance r , from an atom at the reference point of origin.
- Peak height*- The peak height refers to the co-ordination number, and determines the average number of nearest atoms.
- Peak width*- The peak width refers to the dynamic variation between atoms and lattice distortion.

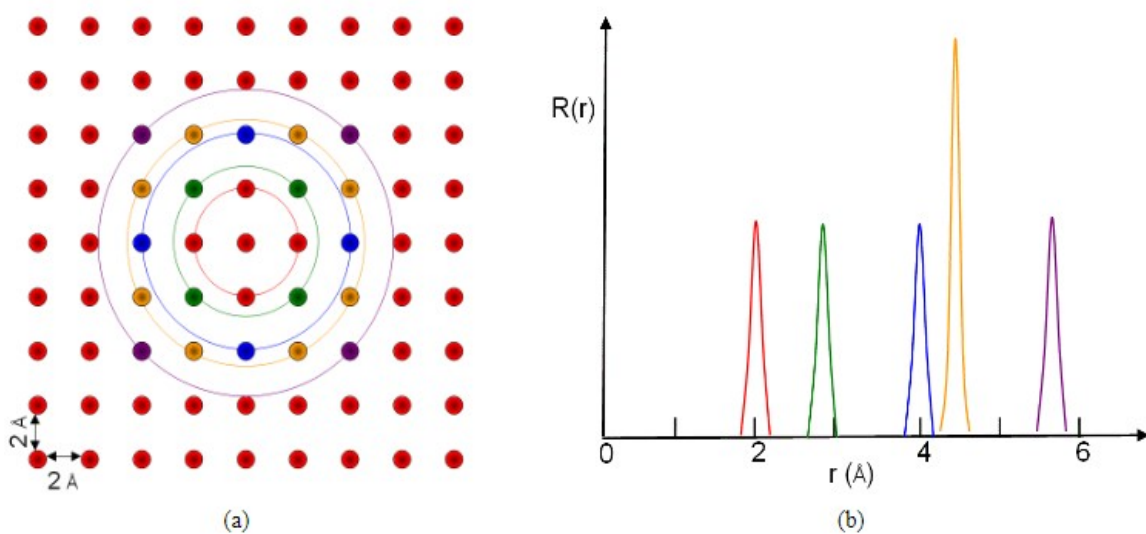


Fig.1.5: (a) Schematic illustration of generation of pair neighbors the origin atom and (b) corresponding peaks in radial distribution function.

10.2 Application of PDF in nano-materials-

Properties of nano materials depend on the local atomic arrangements of atoms which leads to formation of local structures. This localized structures has significant effects on the local nano grains. Structure change to influence in nanomaterial properties, because of their nano grains. Fundamental mechanisms knowledge is very important of the nano scale structure for PDF analysis. It is essential to understand these local structures for better understanding nano-materials for multifunctional applications. Conventional XRD techniques are very difficult to determine this nano structure because of their broad Braggs peaks. If the particle size of the nano structure become reduce,[19] as a reflected in the X-ray diffraction profile get much broadened. This local structural information's can be determined by considering both Braggs peak as well as diffused peaks. Pair Distribution Function (PDF) [21]. Technique is basically considered both Braggs peak as well as diffused peaks from total scattering. In such case the detailed structure knowledge of these nano crystalline materials can be determined from PDF technique. PDF provides local structural information's based on total scattering i.e diffuse scattering along with Bragg's diffraction are both considered. To get overall information to solve structural complexity of the nano materials for better structure-property relation using PDF technique.

1.11 Future transport benefits

Nanotechnology promise to offer of developing multifunctional materials that will give To making and maintaining Vehicles is lighter smarter and safer and more efficient.This technology also using aircraft spacecraft and shipping and many more. in additional nanotechnology offer various way to improve the transportation infrastructure like nano engineering materials in automobile production including polymers nanocomposites structural part high power rechargeable battery system, Thermo electronics material for temperature control lower rolling resistance tires, high efficiency semiconductor and low cost electronics device, thin film use in solar panel and fuel additives it also improve catalytic converter for clear exhaust and extended range. Nano engineering of aluminum, steel, asphalt, concrete and other cementenios material They are recycle forms of our, great promising in terms of improving the performance, resiliency and longevity of highway and transport infrastructure component while reducing their life cost cycle. Nanoscale sensor is use in cost effective continuous monitoring of the integrity structure and high-performance bridges, Tunnel, rails, parking structure and pavement. Nano scale sensor are used in communication devices, other innovations enable by nano electronics which can also support to boost transportation infrastructure that can communicate with vehicle base system, that helps to driver for maintaining lane position, and avoid the collision Between the vehicles, Also adjust travel route to avoid congestion and improve driver interface. The game changing benefits from the use of nanotechnology lightweight, High Street, high efficiency that

material would apply to almost any of the transportation vehicles. For example it has been estimated that the percentages of weight of the commercial jet aircraft by reducing 25% of full consumption by 16%. Analyze perform for NASA has include that the development of use of advantage nanomaterial which twice the strength of conventional composite would reduce the total weight of launch vehicle 63%. Not only could this save the significant amount of energy need to launch spacecraft into orbit but it radius the development of single stage of orbit launch vehicles further reducing the cost of launching, increasing reliability of the vision, and opening that door for new concepts for satellite launching. New concept Capable for innovation into traditional infrastructure material, such as self repairing structure or transmit energy.

1.12 Types of Nanoparticles

Nanoparticles make classified following four criteria (Fig 1.6): morphology, composition, nature and dimensionality [18].

Origin- natural, anthropogenic (e.g. Silver, gold, iron)

Homogeneity- Homogeneous, Heterogeneous (e.g. gold, platinum and palladium catalyst)

Nature-Organic, inorganic, Hybrid (e.g. graphene, carbon nanotube)

Dimensionality- Below 100nm to above 100nm

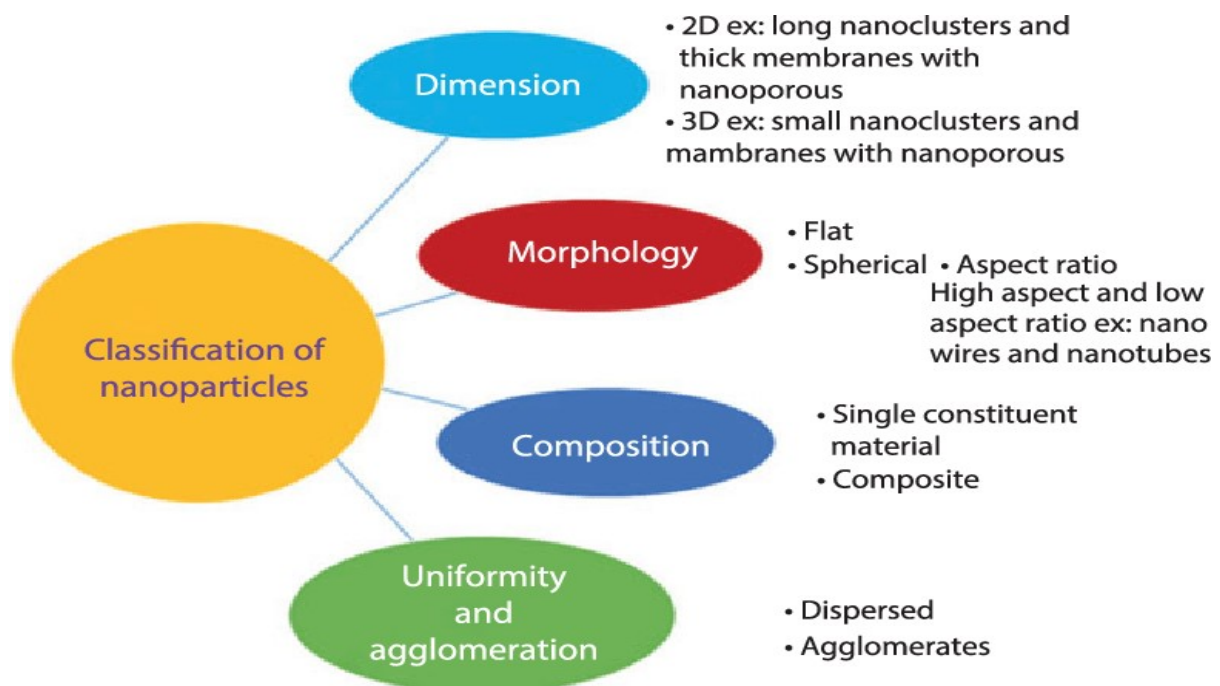


Fig.1.6: Classifications of nanoparticles according to their morphology, composition and dimensionality.

The first classification derived by the MPs base on their nature.

- Atmospheric (biogenic, geodetic, or pyrogenic)
- Anthropogenic (incident and engineering)

The second classification refers to homogeneity in terms of dimension and chemical composition which is divided into homogeneity and homogeneous phase.

The third classification attend to their nature like organic, inorganic or hybrid. According to inorganic nature plasmonic (silver and gold), magnetic NSP (Fe_3O_4), semiconductor (ZnS) and metal oxide (ZnO , TiO_2) are present in case of inorganic NPS liposomes Carbons nanomaterials are found.

The last criteria is the most popular and take into account the diamonds in which double classification is dependent on the dimension which is above 100 nm. In the Royal Society of chemistry and Royal Academy of engineering in 2004 estimated 4 types of nanostructure which is below 100 nm dimensions.

- Zero nanoscale dimension (nanostructures material)
- One nano scale dimension (nanometrics surface)
- Two nanoscale dimension (carbon nanotube)
- Three nanoscale dimension (Fullerene)

However above 100 nm nanostructures describe below [fig1.7].

- Zero dimension 0D (quantum dots)
- One dimension 1D (nanowire)
- Two dimensions 2D (coating)
- Three dimensions' 3D (nanopores material)

Both classification are complementary and closely relate to each other, In both categories we could find disagreement for a specific nanoparticle type. Who share different dimensions. In this thesis the classification of nano particles consider above 100 nm dimension.

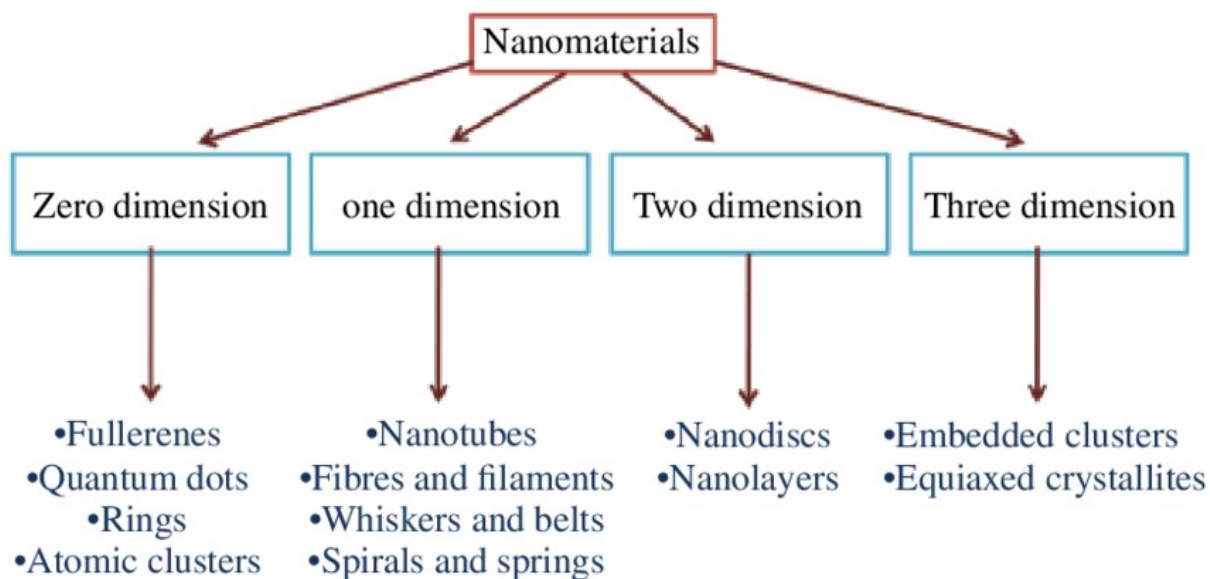


Fig1.7: classification of nanomaterials

1.12.1 Three-dimensional nanomaterials (3-D)

Bulk material not confined in any direction in the nanoscale. These materials are characterised by having three arbitrary dimension which is above 100 nm. material involves the presence of features at the nanoscale or in terms of nanocrystalline structure. But the bulk material can make of a multiple by small particle and arrange of nanosize crystal, in different orientation. The presence of feature at the nanoscale can contain dispersion of nano particle in 3D dimension. Nanoparticles or bundles of nanowire and nanotube in a multi nano layer. For 3D nanomaterial are fully decorated that electrons.

1.12.2 Two-dimensional nanomaterials (2-D)

In 2D nanomaterials are not confirm by dimension in nanoscale, it is a parade plate like shapes. Two dimension nanomaterial include nano layers, nano fluids, and nanocoating. Integrated in grinding material matrix, Metallics, ceramic or Poly metric hard deposited on substance.

In 2D nanomaterials can be made of liquid structure or uniform. it is made up colourful chemical composition and use in a sub case or in multi-layer structure. In case of 2D [23] materials the electrons conductivity will be confirmed across the delocalised plane from the particular distance.

1.12.3 One-dimensional nanomaterials (1-D)

In one dimensional nanoscale that is outside the range that's leads to shape like needle. In 2D materials include Nanotube, nano rod and nanowire. For 1D [22] nanomaterial can be in form of single crystal or polycrystalline with chemical pure or impure, accountant within another medium metallic ceramic, or Poly metric present for one the material electrons confirm occur

in 2D. For only materials electron confines into 2 directions whereas delocalize electrons take place among the long axis of nanowire, rod, and tube.

1.12.4 Zero-dimensional nanomaterials (0-D)

Within all dimensions' material are measure in nanoscale (no dimension or larger than 100 nm). the most common presentation of zero dimensional material are nanoparticle can be in form of liquid or unformed, single crystalline or Poly crystalline are composed by single or multi chemical reaction with the help of chemical reaction it's forms colourful shape, in corporate in a matrix and metallic ceramics r in zero dimension materials. The confirmation for all the nano material in nanoscale is an electron is in the 3D space, No electron delocalise found.

Referance-

- [1]. Sudha, Parappurath N., et al. "Nanomaterials history, classification, unique properties, production and market." *Emerging applications of nanoparticles and architecture nano structures*. Elsevier, 2018. 341-384.
- [2]. Sharma, Ved Prakash, et al. "Advance applications of nanomaterials: a review." *Materials Today: Proceedings* 5.2 (2018): 6376-6380.
- [3]. Glezer, A. M. "Structural classification of nanomaterials." *Russian Metallurgy (Metally)* 2011.4 (2011): 263-269.
- [4]. Rizwan, M., et al. "Types and classification of nanomaterials." *Nanomaterials: Synthesis, Characterization, Hazards and Safety*. Elsevier, 2021. 31-54.
- [5]. Martin, Charles R. "Membrane-based synthesis of nanomaterials." *Chemistry of materials* 8.8 (1996): 1739-1746.
- [6]. Xu, Hangxun, Brad W. Zeiger, and Kenneth S. Suslick. "Sonochemical synthesis of nanomaterials." *Chemical Society Reviews* 42.7
- [7]. Yu, Hai-Dong, et al. "Chemical routes to top-down nanofabrication." *Chemical Society Reviews* 42.14 (2013): 6006-6018.
- [8]. Kang, Yijin, et al. "Shaping electrocatalysis through tailored nanomaterials." *Nano Today* 11.5 (2016): 587-600.
- [9] Khan, Firdos Alam. "Synthesis of nanomaterials: methods & technology." *Applications of Nanomaterials in Human Health*. Springer, Singapore, 2020. 15-21.
- [10]. Rizwan, Md, et al. "Ecofriendly application of nanomaterials : nano bio-remediation." *Journal of Nanoparticles* 2014 (2014).
- [11]. Lahann, Joerg. "Nanomaterials clean up." *Nature nanotechnology* 3.6 (2008): 320-321.
- [12]. Khan, Haseeb A., and Rishi Shanker. "Toxicity of nanomaterials." *BioMed research international* 2015 (2015).
- [13] Nikaeen, Ghazal, Sepideh Abbaszadeh, and Saeed Yousefinejad. "Application of nanomaterials in treatment, anti-infection and detection of coronaviruses." *Nano medicine* 15.15 (2020): 1501-1512.
- [14] Khan, Haseeb A., and Rishi Shanker. "Toxicity of nanomaterials." *BioMed research international* 2015 (2015).
- [15]. Foulkes, Rachel, et al. "The regulation of nanomaterials and nanomedicines for clinical application: Current and future perspectives." *Biomaterials science* 8.17 (2020): 4653-4664.
- [16]. Lee, Ju Min, et al. "Exciton dissociation and charge-transport enhancement in organic solar cells with quantum-dot/N-doped CNT hybrid nano materials." *Advanced Materials* 25.14 (2013): 2011-2017.

- [17] Siddique, Sarkar, and James CL Chow. "Application of nanomaterials in biomedical imaging and cancer therapy." *Nanomaterials* 10.9 (2020): 1700.
- [18]. Tao, Feng, et al. "Carbon nanotube-based nanomaterials for high-performance sodium-ion batteries: Recent advances and perspectives." *Journal of Alloys and Compounds* 873 (2021): 159742.
- [19]. Christiansen, Troels Lindahl, Susan R. Cooper, and Kirsten MØ Jensen. "There's no place like real-space: elucidating size-dependent atomic structure of nanomaterials using pair distribution function analysis." *Nanoscale Advances* 2.6 (2020): 2234-2254.
- [20]. Banerjee, Soham, et al. "Improved models for metallic nanoparticle cores from atomic pair distribution function (PDF) analysis." *The Journal of Physical Chemistry C* 122.51 (2018): 29498-29506.
- [21]. Juelsholt, Mikkell, et al. "Surfactant-free syntheses and pair distribution function analysis of osmium nanoparticles." *Beilstein journal of nanotechnology* 13.1 (2022): 230-235.
- [22]. Zhong, Yi, et al. "Interface engineering of heterojunction photocatalysts based on 1D nanomaterials." *Catalysis Science & Technology* 11.1 (2021): 27-42.
- [23]. He, Zuoli, et al. "1D/2D Heterostructured photocatalysts: From design and unique properties to their environmental applications." *Small* 16.46 (2020): 2005051.
- [24]. Sinha, S., H. Kim, and A. W. Robertson. "Preparation and application of 0D-2D nanomaterial hybrid heterostructures for energy applications. " *Materials Today Advances* 12 2021.
- [25]. <https://www.intechopen.com/chapters/46953>
- [26]. <https://link.springer.com/article/10.1007/s10529-015-2026-7>

Chapter 2: General Overview on BaTiO_3

2.1 Introduction of BaTiO₃ :

Barium titanate has been the first piezoelectric and ferroelectric ceramic which is developed for remarkable operation and it use in extensively purposes, especially it is used for high permeability dialectic in multilayer ceramic capacitor and as Semiconducting material with positive temperature measure of resistivity temperature (PTCR) in transistor. At room temperature barium titanate adopts in tetragonal phase the type of structure is tetragonal with the high permeability and ferroelectric. When it transform tetragonal to cubic, at piezoelectric state the Curie temperature is approximately 130 degrees I. electric field in piezoelectric materials depends on the Curie temperature [1].

The operation of a high electric field the polarization of the ferroelectric discipline along the direction of the external field within the grains. The poled state remain indeed after the junking of field, therefore indeed the ceramic despite its polycrystalline nature it's behave like a single dimension showing useful ferroelectric and pyroelectric Property. In fact unpoled ceramic are not piezoelectric Lee active because the donation of the grains wood aimlessly acquainted, on the whole cancel out each other. The advantages was significant for the large scale production an operation or ferroelectric accountant, as ceramic are cheaper than single charge and they are fact through inferior of those of single diameters can more friendly acclimatised.

The resistivity of barium titanate convert the tetragonal to Cubic phase transition temperature has lead to several operations as Over current and tone regulating heaters is needed. This miracle is only deserved theme polycrystalline barium titanate with the polarisation of ferroelectric displace line, modifying the bonding with the electronics transport across in the grain boundary.

Table 2.1: The important properties of BaTiO₃

| Sn | PROPERTY | VALUE | REFERANCE |
|----|-------------------|------------------------------|-----------|
| 1 | Band gap | 3.2eV (300k, single crystal) | [10] |
| 2 | Refractive index | $n_o=2.412$; $n_e = 2.360$ | [11] |
| 3 | Curie temperature | 120 to 130 °C | [12] |
| 4 | Polarization | 0.26 C/m ² | [13] |
| 5 | Melting point | 1625 °C | [14] |
| 6 | Density | 6.02 g/cm ³ | [15] |
| 7 | Young's Modulus | 67 Gpa | [15] |

| | | | |
|---|----------|--------|------|
| 8 | Hardness | 5 Mohs | [15] |
|---|----------|--------|------|

2.2 Crystal Structure, nono- stoichiometric and Defect Chemistry of BaTiO₃

The barium titanate perovskite has different crystallographic variation depending on temperature at higher temperature it's from cubic structure. This is centro symmetric structure with Ba⁺ at the corner and Ti⁺ at the center and oxygen (O⁺) at the face in crystal structure. In octahedral structure titanium iron is coordinated by 6 oxygen ion within structure and Ba has dodecahedral coordination [2].

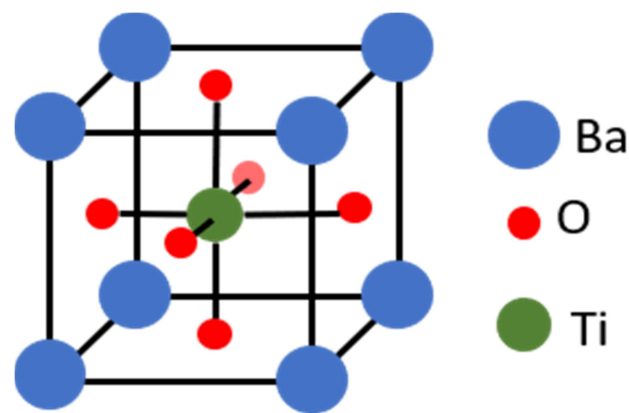


Fig.2.1: Unit cell of BaTiO₃

At the Curie temperature, $T_C = 120\text{--}130^\circ\text{C}$, it turns from the high temperature Para electric cubic form (C) to the ferroelectric tetragonal structure (T). On further cooling 2 other ferroelectric phase are observed, orthorhombic (O), below $5\text{--}151^\circ\text{C}$, and rhombohedral (R), below -80 to 90°C .

In BaO-TiO₂ Have at least 9 compounds which have been proven to be useful in Electro ceramic material, with the most important perovskite barium titanate is use in MLCC and PTC hour devices. Below 1460°C BaTiO₃ process the perovskite structure at higher temperature. At higher Temperature hexagonal face polymers with non perovskite structure appear. The perovskite transition temperature is very sensitive to the presence of acceptor dopant. In the deformation of cubic unit cell along the edge ([001], tetragonal), along a face diagonal ([011], orthorhombic), or along a body diagonal ([111], rhombohedral) Likewise, the orientation of the electrical dipole is [001], [011] and [111] for the T, O and R modifications, respectively. At room temperature the ratio c/a of the lattice parameters of the tetragonal cell ($a = b, c > a$) is 1.011,

2.3 introduction BCZT :

Lead- based materials (PZT) use in last few years due to their outstanding property like dialectic, piezoelectric, and ferroelectric, for operation in energy storage. Piezoelectric

material converts mechanical energy into Electrical energy or vice versa. They are widely using in capacitor, acuter, transistor devices. Over the last few years, lead based PZT use in piezoelectric material. However lead based material content lead oxide more than 60% therefore various environmental problem causes like headache, anemia, nerves, brain, and kidney damage etc. that's why lead based pizoceramic has been replace by lead free materials like BZT recent year we have great effort for made to develop lead free piezoelectric material.

In 2009, Liu and Ren(6) reported Ba_{0.85} Ca_{0.15} Zr_{0.10} Ti_{0.90} O₃(BCZT) Ceramic have excellent dialectic and electromechanical property add the morphemic phase bound daddy the first published confirmation BCZT [3,4] complex compound was grounded on solid state reaction at height (Calcination at 1350 C and sintering between 1450- 1500 C) temperature due to its simplicity and capability to enhance dielectric, ferroelectric, and piezoelectric performance.

2.4. Dielectric Properties:

All sample have a broad range of dialectic value associate with tetragonal to cubic phase transition the dielectric loss of all the sample decreases gradually when the temperature increases after certain value of temperature the value remains constant, and after that it increases. The overall dielectric measure from 20 Hz to 10 MHz [5]. The dielectric property directly varies with surface area of materials.

C=Capacitance (F)

A= area of plate (m²)

D= Thickness of plate (m)

K= Dielectric constant

ε₀= Permittivity of free space (8.854× 10⁻¹² F/m)

$$C = \frac{k\epsilon_0 A}{d}$$

2.5 Purpose of Doping

Undoped barium titanate ceramic have their limited application in dielectric, capacitance, transistor and electronic devices. it shows a significant temperature dependence. The development of BaTiO₃ is a base material and their use industrial application has been derived by the needed. chemical modification represent the most basic and common approach in the phase transition and mechanical milling is a one of easy method for doping calcium and zirconium into it, These two method are most common approach for tuning the face transition and the property for barium titanate another ferroelectric perovskite. Pure BaTiO₃ have relatively low dielectric value, so to overcome this problem doping is suggested, so ca²⁺ and Zr⁴⁺ can be introduced into the BaTiO₃ [6]. Even a very small amount of doping can considerably modify functional properties like the electrical conductivity and the domain wall

mobility or dielectric. When some amount of iron is present in lattice it's more appropriate for formation of solid solution. Chemical modification is essential to fresh transition with temperature and it's particular to lower curie temperature around room, the modify nature of the phase transition is formation of solid solution. Which is located compositional function with minimise the polar correction length. Diffuse phase transition over a relative large temperature range leading to broad permittivity peak. Doping is also needed to impact the material and number of characterization properties for making and reliability under operational condition. it is also known as the permeability and piezoelectric activity of barium titanate ceramic with grain size less than $1\mu\text{m}$ [7]. for the strategy commonly use for increasing dielectric property in the capacitor application with core shell grains, which combines the chemical modification with the control of microstructure and formation of compositional gradient. Dielectric and piezoelectric properties can also be controlled by modification of nanostructure in particular direction.

- (1) Simple in structure and composition.
- (2) Doping provided high stability and easy to adopt properties to the specific application. For making pevroskite and nanostructure solid solution is adopted.
- (3) In the case of ceramics relatively cheap processing and simple especially.
- (4) In core application high competitors are have.

References:

- [1]. Jia, C. L., et al. "Introduction and characterization of interfacial defects in SrRuO₃/BaTiO₃/SrRuO₃ multilayer films." *Journal of crystal growth* 247.3-4 (2003): 381-386.
- [2]. Tripathi, A. K., R. Sekar, and P. K. C. Pillai. "XRD studies of a BaTiO₃: PVDF composite." *Materials Letters* 9.1 (1989): 24-28.
- [3]. Nayak, Suryakanta, Tapan Kumar Chaki, and Dipak Khastgir. "Development of poly (dimethylsiloxane)/BaTiO₃ nanocomposites as dielectric material." *Advanced Materials Research*. Vol. 622. Trans Tech Publications Ltd, 2013.
- [4]. Verma, Ritesh, et al. "Structural, optical, and electrical properties of vanadium-doped, lead-free BCZT ceramics." *Journal of Alloys and Compounds* 869 (2021): 159520.
- [5]. Chu, Bao-Jin, et al. "Electrical properties of Na_{1/2}Bi_{1/2}TiO₃–BaTiO₃ ceramics." *Journal of the European Ceramic Society* 22.13 (2002): 2115-2121.
- [6]. W. Liu, X. Ren, *Phys. Rev. Lett.* 103, 257602 (2009)
- [7]. Z. Wang, J. Wang, X. Chao, L. Wei, B. Yang, D. Wang, Z. Yang, *J. Mater. Sci. Mater. Electron.* 27, 5047 (2016)
- [8]. J.P. Praveen, T. Karthik, a.R. James, E. Chandrakala, S. asthana, D. Das, *J. Eur. Ceram. Soc.* 35, 1785 (2015)
- [9]. M.a.Rafiq, M.n. Rafiq, K. VenkataSaravanan, *Ceram. int.* **41**, 11436 (2015)
- [10]. Suzuki, Keigo; Kijima, Kazunori (2005). "Optical Band Gap of Barium Titanate nano particles".
- [11]. Tong, Xingcun Colin (2013).
- [12]. Vincenzo Buscaglia, Maria Teresa Buscaglia, and Giovanna Canu, *BaTiO₃-Based Ceramics: Fundamentals, Properties and applications*
- [13]. Shieh, J.; Yeh, J. H.; Shu, Y. C.; Yen, J. H. (2009-04-15). "Hysteresis behaviours of barium titanate single crystals".
- [14]. Galasso, Francis S. (1973). *Barium Titanate, BaTiO₃*
- [15]. Barium Titanate(BaTiO₃) - Properties and applications, a ZO materials.

Chapter 3: Literature review

Literature Review

P Jaimeewong.etal. [1] prepared $\text{Ba}_{0.85}\text{Ca}_{0.15}\text{Zr}_{0.1}\text{Ti}_{0.9}\text{O}_3$ (BCZT) powders via conventional mixed oxide and sol-gel auto combustion methods. The stoichiometric amounts of the Aldrich powders were mixed by ball milling for 24 hrs in ethanol medium. The sample were dried at 120°C for 24 hrs. The dried powders were heated at 1200°C for 2 hrs with a heating as well as cooling rate of $5^\circ\text{C}/\text{min}$. pure BCZT has tetragonal phase, and after splitting diffraction peak could be the reflection of a rhombohedra structure. However Combustion method prepared powder increased the dielectric properties while the ferroelectric properties decreased.

Z hanani et al. [2] used $\text{Ba}_{0.85}\text{Ca}_{0.15}\text{Zr}_{0.1}\text{Ti}_{0.9}\text{O}_3$ (BCZT) Compound, for observe excellent, dielectric, ferroelectric and piezoelectric properties in this ceramic. All the properties are present in this material is greater than commercially available lead base materials. Sol gel method use for synthesis of Aldrich BCZT nano-powder, at the lower temperature, 25 80, and 160°C . The x-ray diffraction demonstrated that all BCZT sample are crystalline in a perovskite phase with a tetragonal structure at room temperature, and also increasing heat treatment with decrease in gains size enhance the dialectic and ferroelectric property of BCZT ceramic.

Frattini a et al. [3] BCZT perovskite where prepared by mixed oxide system by the conventionally high energy ball milling, with the nominal composition of $\text{Ba}_{0.89}\text{Ca}_{0.11}\text{Zr}_{0.10}\text{Ti}_{0.90}\text{O}_3$. The preparation was done into planetary ball milling with high energy transfer during 4 hours into a Zr jars. differential thermal analysis (DTA) and Thermogravimetric analysis (TGA) used to measure for atomic bond and weight loss Due to heating at temperature from 20 to 1200°C at 10 see per minute of hitting rate at normal atmosphere. Two weight percentage PVB was added as a binder for making plate with uniaxial pressure mechanical machine make bullets with pressed at 200 Mpa. The powder sample was converted at constant heating rate 5 degrees per minute in a Theta Dilatronic Dilatometer. Different bullets are synthesise at 1250°C , 1300°C and 1400°C . The structural analyse of the sample was performed by XRD. And surface morphology detected why FESEM. The results shows that the increase of temperature leads to enhance the electric properties.

Xu, Kangli, et al [4] uses $\text{Ba}_{0.85}\text{Ca}_{0.15}\text{Zr}_{0.1}\text{Ti}_{0.9}\text{O}_3$ (BCZT) ceramic doped with MgO cumulative Was synthesis bye solid state reaction. The phase identification of the sample used by Xrd analysis and show tetragonal face of the perovskite structure. Using same micrograph reveals that the lower grain size is up to 0.50 composition. As compared with the pure tetragonal BCZT ceramic, the transfer of phase with the addition of MgO, orthorhombic and tetragonal face can be detected. The composition of BCZT 0.5 wt of

MgO with high thermal stability, an energy storage. Thus energy storage effectiveness has increases from 92.60 to 97.08 at the temperature range from 22 to 120 C.

Mittal s, K. Chandramani et al [5] $\text{BaCO}_3(99.9)$, $\text{CaCO}_3(99.9)$, $\text{ZrO}_2(99.8)$, $\text{TiO}_2(99.8)$ were take as the Aldrich raw powder, and mixed with counted amount to their stoichiometry in $\text{Ba}_{0.85} \text{Ca}_{0.15} \text{Zr}_{0.1} \text{Ti}_{0.9} \text{O}_3$ (BCZT). Mixing is done into planetary ball milling with 800 rpm for 20 hours. After the mixer was put in the heater for 24 hours to get dry. The dry sample is use for making green plate and calculated at 1200 C for 4 hours heating, the heating rate of the sample is 5 C per minute. The XRD result so that the composition of ceramic is set up to the tetragonal phase at room temperature. The pyroelectric measure with the increase in temperature with increasing value and also measure decreases temperature for all the sample as vice versa.

Saparjya et al. [6] used of Gadolinium (Gd) on $\text{Ba}_{0.85} \text{Ca}_{0.15} \text{Zr}_{0.1} \text{Ti}_{0.9} \text{O}_3$ (BCZT) ceramic Prepared by high temperature (1300 C) In solid state reaction. The X-Ray Diffraction Pattern at room temperature of the sample are confirmation that single phase tetragonal structure. The entire sample are mixed in air with the help of motor for 2 hours, And dry slowly by evaporation method. The samples are carried out into heater for calcination process that 1250 C for 4hours' duration. The dialectic is carried out in temperature dependence environment, in the study phase transition was observed. It can also be Measure that losses of maximum value are lower after the addition of GD to the sample, which is favourable for electronics operation. From diffusive compound it set up with the addition of Gdis 0.1% the number vaccine variation is reducing oxygen in this experiment. Due to reduction of oxygen the dielectric value also reduces.

M. Goune et al [7] To understand the grain size distribution on the electric plate of lead free BCZT ferroelectric is great. The lead free material BCZT ceramic has important properties for the fabrication of nano electronics bias by virtual of their excellent dielectric, ferroelectric and piezoelectric property. BCZT was prepared by solve thermal process with low temperature starting with 20 C to 1200 C. The dielectric constant measure was in the range of 5370 to 9646 and dielectric loss was by 70% of measure value. In conclusion, they are 3 types of largely ceramic is present with different grain size and enhance dielectric property was successfully prepared by low temperature sintering.

Fangbinwei et al.[8] study, environmentally friendly Bi-substituted($(\text{Ba}_{0.85} \text{Ca}_{0.15})_{1-3x/2} \text{Bi}_x)(\text{Zr}_{0.1} \text{Ti}_{0.9}) \text{O}_3$ (BCZT- xBi) ferroelectric pottery with $x = 0 - 0.08$ were prepared using a solid- state sintering system. The dielectric, Electro-caloric sample of the lead free bed ceramic was completely delved. The hysteresis of the S-P angle in undoped BCZT ceramic came significant properties with an increase in temperatures because of activation of conductivity. In case of $x=0.8$ Composition ceramic the conductivity is increase with temperature. Therefore, we only estimated the temperature which is dependent ferroelectric

and electromechanical sample of the BCZT – xBi ceramic with $x = 0.02, 0.04$ and 0.06 composition. The ferroelectric and electromechanical sample measure over the temperature range of 30 to 120 °C. In case of ceramic with $x = 0.02$ and 0.04 the hysteresis peak first narrow and increasing with temperatures peak become broaden. With increase in the Bi component from 0.02 to 0.06 the thermal stability is better. Further change in ratio from 0.49 to 0.06 reduction of stability. The ceramic shows good thermal stability at 0.06 range, and electrostatic and electro caloric promising seeker to gain excellent electrostatic response by adding the field strength.

Ismail Khmiri et al (9) study of $(\text{Ba}_{0.99}\text{Ca}_{0.01})(\text{Zr}_{0.2}\text{Ti}_{0.8})\text{O}_3$ (BCZT) and unravel $(\text{Ba}_{0.99}\text{Ca}_{0.01})(\text{Zr}_{0.2}\text{Ti}_{0.8-x}\text{Mnx})\text{O}_3$ (BCZT- xMn) pottery was successfully carried out by the solid- state method. The extra pattern of BCZT and BCZT – xMn ceramic show diffraction peak at 45° , in two peak we see some changes in peak position (002) and (200) which reflect in the tetragonal structure of BCZT ceramic. Pure ceramic and doped ceramic records for a frequency range from 20 to 1 MHz. It shows that decrease in frequency increase with dielectric permittivity. For BCZT ceramic maximum temperature is close to the room temperature and slightly dissipation at outside the room. The quality of Mn increase the dielectric value increase with reduce temperatures and shift occurred with maximum permittivity. It is also noted that there is a low dispersion of the permittivity for $T \leq T_m$ (T_m maximum value of the temperature) and the losses of dielectric decrease with temperature for all samples. The value of this parameters increase if Mn concentration increase, which suggest that Mn doping in BCZT ceramic the Diffusion of ceramic phase transition and minimise the dielectric loss.

Ripank Biswas et al [10] study pair distribution Function (PDF) of carbonation of barium titanate in nano scale. Commercially available tetragonal BaTiO_3 milled in ball milling, and to study the local atomic structure and phase transformation behaviour with temperature. Ball milling process continues for 90 hrs, when BT was exposed to open air it was carbonated. Local structure or atomic distribution was obtained from PDF analysis. Due to calcinations barium carbonate (BC) peak was observed, and C-O and Ba-C pair distance observed from PDF. TEM analysis revealed diameter range 15 - 50 nm. During heating at 900 °C temperature BT transformed into tetragonal and cubic phase via monoclinic phase. The presence of carbon in the form of BC in BT sample conform by PDF. Off-centring Ti atom was clearly observed from PDF. C-O and Ba-C pair distance 4.45 Å and 5.00 Å appeared in 90 hrs milling BT powder. Wt% of BC phase initially reduce and completely disappeared at 900 °C.

References:

- [1]. "Jaimeewong, Piyaporn, et al. "Comparative study of properties of BCZT ceramics prepared from conventional and sol-gel auto combustion powders." *Integrated Ferroelectrics* 175.1 (2016): 25-32".
- [2]. "Hanani, Zouhair, et al. "Structural, dielectric, and ferroelectric properties of lead-free BCZT ceramics elaborated by low-temperature hydrothermal processing." *Journal of Materials Science: Materials in Electronics* 31.13 (2020): 10096-10104".
- [3]. Frattini, a., et al. "BCZT ceramics prepared from activated powders." *Procedia Materials Science* 1 (2012): 359-365.
- [4]. Xu, Kangli, et al. "Temperature-stable MgO-doped BCZT lead-free ceramics with ultra-high energy storage efficiency." *Journal of alloys and Compounds* 829 (2020): 154516.
- [5]. Mittal, S., and K. Chandramani Singh. "Size Effect of nanoscale Powders on the Polarization of the BCZT Piezoceramic: a Pyroelectric and Fatigue Perspective." *Integrated Ferroelectrics* 205.1 (2020): 122-130.
- [6]. Saparjya, S., et al. "Effect of Gadolinium on the structural and dielectric properties of BCZT ceramics." *Phase Transitions* 93.2 (2020): 245-262.
- [7]. Hanani, Zouhair, et al. "Enhancement of dielectric properties of lead-free BCZT ferroelectric ceramics by grain size engineering." *Superlattices and Microstructures* 127 (2019): 109-117.
- [8]. Wei, Fangbin, et al. "Structure, dielectric, electrostrictive and electrocaloric properties of environmentally friendly Bi-substituted BCZT ferroelectric ceramics." *Ceramics international* 47.24 (2021): 34676-34686.
- [9]. Khmiri, ismail, issa Kriaa, and Hamadi Khemakhem. "Effect of Mn doping on structure, the dielectric and electric properties of BCZT ceramics." *applied Physics a* 127.4 (2021): 1-8.
- [10]. Islam, Sahanoor, Ripan Kumar Biswas, and Jiten Ghosh. "Use of high temperature X-ray diffraction and pair distribution function for the study of carbonation characteristics of Barium Titanate at nanoscale." *Micro & Nano Letters* 14.11 (2019): 1204-1207.

CHAPTER -3 Experiments

4.1 Experimental Set up:

In this paper, i used Fritsch ball milling machine for homogeneous mixing of BCZT, for this purpose, we used various types of instruments and tools. Such as, for homogenous mixing purpose Fritsch ball milling, for dielectric Wayne Kerr 6500B for characterizing purpose we use various instruments such as Rigaku-UltimaiV (XRD analysis), HITACHI SU8020 (FESEM analysis) etc., which is given below.

4.2 Material Synthesis:

Various equipment are use to make BCZT from BaCO_3 , CaCO_3 , ZrO_2 and TiO_2 nano power.

4.2.1 Planetary ball milling: -

Ball milling contains of a hollow cylindrical shell it's rotate about its own axis [fig.3.1]. The sell axis maybe either horizontal or tilt at a small angle to the horizontal plane. The sell contents partially filled with zirconium balls. The grinding mechanism is done with the ball which may be made of steel, stainless steel or rubber. The length of the meal is approximately equal to its diameter. The ball occupys about 35 to 55% of total volume. The inner surface of cylindrical shell is usually lined with and corrosion resistant material such as stainless steel or rubber. The diameter of ball use in between 12 mm and 125 mm. the rotating speed of the shell is 52 to 500 rpm and large ball milling the shell maybe 3 meters in diameter and 4.5 m in length. The mechanism of ball milling is when the shell rotates with Zirconium ball high energy impact on the sample and break the sample and uniform grinding particles produced.



Fig.3.1:- Planetary Ball Milling (Fritsch)

Advantages of the Ball Mill-

- Low cost of installation.
- Low cost of power consumption.
- Degree of hardness for all sample is suitable.
- It can be used for grinding of certain explosive material which can be used with an inert normal atmosphere.

Disadvantaged-

- It's time taking process and non uniformity in the particle sizes.

4.2.2 Furnace:- Instead of using pilot light in furnace electric use in that position, an election start ignition the heat generated. In gas power burner furnace, the ignition activates heating element that contains conductive coils. When current passes through the coils they start heating, and air flow to control it. Use high heat of thermostat, high heating coils turn on. In electric furnace heart goes up to 2000 C, and it takes less time to reach highest value. In this experiment we used Naskor furnace, and sample heated up to 1200 C with control environment and increase heat rate 5C/ min, it stat for 1 hr after that it cool down with same rate of heating.

4.2.3 Sonicator bath :-

Sonication is use generally into sound waves to colloidal particles in a solution. It transmitted an electrical signal to a mechanic vibration to separate accumulates particles. The disruption can mix solution, and dissolved solids into a liquid, such as use water, polyvinyl alcohol, and acetone as dispersed solution. To remove dissolved gases from liquids salt added into it. Before FTIR testing, sonication breaks [fig.3.2] molecules and disintegrated, so that particle cannot accumulate and capture sharp/single particle image.



Fig.3.2:- Sonication bath

4.3 Materials Characterization tools :-

Using –Ray diffraction (XRD, Rigaku) The phase constituents of Ca and Zr composites were identified) with Cu Ka with a scanning speed of 5° per min. The microstructures were characterized by a XRD, PDF Field Emission Scanning Electron Microscopy (FESEM) and dielectric measure by Wayne Kerr 6500B etc are describe in given below.

4.3.1 X-Ray Diffraction (XRD).

In 1895, x-ray is discovered by Roentgen. From the year 1912, the application of x-ray has started when the wave nature of x-ray was recognized from the x-ray diffraction by any crystals. X-ray diffraction by the different set of planes has been applied to identify crystal structures. The structural characterization of synthesized samples is observed results by X-ray Diffraction peak on the sample. XRD pattern was taken using Cu & Ka radiation (1.5406\AA) (Rigaku-Ultima-iii, fig.3.3).



Fig3.3- X-Ray Diffratometer (Rigaku Ultima-iii)

The photograph is shown in the figure 3.5 below. The basic theory involved in XRD, the crystal structure analysis is using Bragg's law of diffraction. When monochromatic x-ray fall on the Particle in ceramic crystal, then each of electrons atom act as scattering electrons. In crystal lattice act as a series of parallel reflecting scattering plane. The reflected beam at certain angle from 0 to 180 degree (which is multiplied of constructive interference) .This is called bragg's law, and it is defined by the relation,

$$n\lambda = 2d\sin\theta \dots\dots\dots(i)$$

In this relation “n” indicate the order of diffraction or number of planes. And “d” is spacing between two consecutive planes, λ is wavelength of x-ray, and θ is diffraction angle between source and detector of electron beams. In XRD study of any sample gives a big range of information about the crystal structure average crystalline size and various stress as well as composition about the crystal. Generally, the obtained experimental data of the sample are compared with the standard inorganic crystal structure database (ICSD) to confirm the phase purity of our synthesized samples.

The shift in peak position, one can calculate the changes of d-spacing between plane, which signify the change of lattice constant under inhomogeneous or homogeneous strain. Inhomogeneous strain differs from crystallite to crystallite or within a single crystallite. This causes the peak broadening which increases with sine. This broadening also occurs from the crystalline size effect, but here the broadening is independent of $\sin \theta$. If there is no inhomogeneous strain, the crystallite size, D can be calculated from the Scherrer's formula:

$$D = (k\lambda/\beta \cos \theta) \dots\dots\dots(ii)$$

Where, β is the full width and half maxima (FWHM) of a diffraction peak, k is the Scherrer constant and θ is the diffraction angle [1-3].

4.3.2 FESEM (Field-Emission Scanning Electron Microscope):

I. Principle

Under vacuum condition, the electrons are generated by field emission source are accelerated in a tube. The ray passes through in electromagnetic lens, has a reason of this different type of electrons are release from the tube. A sensor catches the secondary electrons and fall on the sample. As a result an image of the sample is constructed by the intensity of this secondary electrons to the scanning primary electrons beam and eventually the image is display. FESEM is used to identify the morphology and small topography details of a sample. In research work FESEM use in biology, chemical and drugs application. This system to observe the structure of a any crystals which is smaller than one nanometer. The FESEM may illustration to study DNA and organic cells, synthetically polymer and coating on micro chips.

II. Preparation

In order to observe with a FESEM object first made conductive with electrons. In this work we did by sheeting them with a thin layer of carbon. The object must be suitable to survive in high vacuum and should not alter in vacuum. For insulation by losing water, generally polymers are kept they are structured in the same. With cold slush nitrogen or with chemical mixture put on the sample. This particular microscope is for seen of a special cryo unit, where frozen object can be captured for direction in the FESEM observation [fig.3.4]. Chemically fixed material needs first to be washed and dried below the critical point to avoid the damage of fine structure due to pressure put on the sample. The powder sample is first diluted with polyvinyl alcohol or acetone then it is put on a glass, after that it is dried for a few hours then coating is performed. Coating is also performed in a separate device.

III. Source of electrons

In standard electron microscope electrons are generated by heating of tungsten light, by means of current passing through the light and due to high electron passing the temperature rises up to 2800 °C. Over tungsten hair lanthanum hexaboride (LaB6) mounted on top and elections are produced. The advanced election moves into the tube with the velocity of x-ray. And give better resolution images than the conventional device. In field emission (FE) survey Electron microscope have no heating issue because sources employed provide by cooling system. An extremely thin and sharp tungsten used for function as a cathode in front of primary and secondary anode. The voltage between cathode and anode is 0.5 to 30 KV. The electron ray produced by the FE source is about 1000 times lower than the standard microscope, the image quality is better than conventional microscope. As field emission (FE) have extremely high vacuum in the column of microscope the devices present the regularly decontaminates the electron source by the current flash discrepancy to a conventional tungsten. FE tip has Theoretically Stable the vacuum system. Due to the extreme vacuum (8 to 10 Torr) pressure put on the device, the device is regulated decontaminates the electron source by a current flash, and handed vacuum is maintained stable.

IV. image formation

When the primary electron beams fall on the object, the object gets excited and secondary electron beam produces from the object face with a certain velocity which is determined by the levels and angles at the surface of the object. The secondary electrons which are attracted by the corona, with strike the fluorescing glass that produces photons. The position and intensity of the mirror may very depend on the property of secondary electrons. The signal produced by the detector is amplified and transmitted into a video signal that is maintained to a cathode ray tube in the microscope with movement of electron beam. The real time image that appears on the reflected screen. The structure of the surface on the object parallel to the

analogues image formation. A digital image is generated which can be further processing same.



Fig.3.4:- Field-Emission Scanning Electron Microscope (FESEM, sigma, Zeiss).

V. Working principle

1. The “virtual source “at the top represent electron gun, to producing a bundle of monochromatic election.
2. The electric beam is concentrated of a small, thin beam to use for condenser lenses. Here two lens are us, the fast lanes use for control sport size, and second lens use for intensity. The spot size lens generally size range of the final spot strikes on the sample. And second lens changes the size of the spot on the sample, it changing from a wide dispersed pin point spot in beam.

3. The beam is restricted by condenser as a aperture knocking at high angle electrons. It is far from the optical axis and line draw into the centre.
4. When beam strikes the specimen electrons are transmitted.
5. The transmitted electron is concentrated by the objective lens into image.
6. The object and selected area are restricted the beam with metal apertures. The objective apertures enhancing by blocking out high angle diffracted electrons, The area apertures used to examine the periodic diffraction of the electrons by the order of atom in the sample and arrange in proper shape.
7. The images passing through the column in intermediate and projector lens, being enlarge. The electron beam the phosphor image skin and light is generated and allowing the user to see the image.

4.3.3 Fourier Transform Infrared Spectroscopy (FTIR):

Fourier Transform infrared spectroscopy (FTIR) Is a technique in which chemical compositions are determine like organic compounds, Polymers, coating, lubricant, semiconductor materials, gases, natural sample, and inorganic compounds. This technique can use to analyze a wide range of material in thin films, liquids, solids, powder, and fiber. FTIR technique cannot give any quantity information of materials but with relevant standard it can perform. FTIT can be used to analyze the sample whose diameter is 11 millimeters and beyond of 1 micrometer. The FTIR spectrometer is a device in which NIT to FIR broadband spectra are use. FTIR spectrometer collection of all wavelength simultaneously and Fourier transform infra red is use to carry the information, the first collecting an inter-ferogram of a sample signal use as an interferometer. The bond length of compounds is measure in Specific range. Only metallic bonds are detected in FTIR.

i) Principle of operation:

FTIR is based on a interferometer, it's consist of a beam splitter. A fixed mirror that move forward and backwards sententionusly. The ray splitter is made of a special material that transmits half of the radiation and reflect the other half. The source strikes the beam splitter and divided into two parts [fig.3.5]. One part beam transmitted through beam splitter on the fixed mirror and other beam is reflect to beam splitter with the moving mirror. Both the mirror reflect the radiation back to the beam splitter. Half of the radiation is transmitted, and half is reflect. So the one beam passing through the detector and second beam move back to the source.

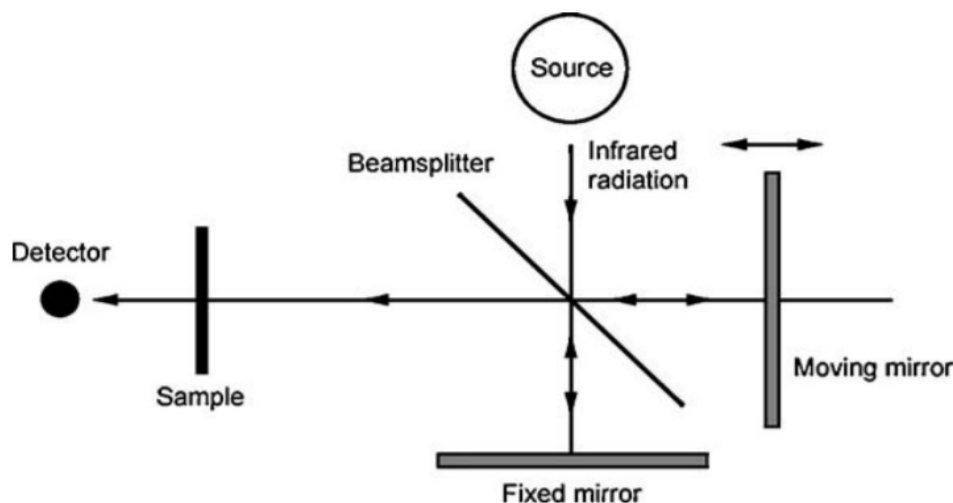


Fig.3.5:- Schematic diagram of the FTIR spectrometer

The beam of infrared ray whose wavelength is 0.7 to 500 μm is concentrated on the sample and reflective optics. Depending on the sample properties. Different quantity of light are absorbed different size of wavelength, this pattern of light absorbed is unique for each compounds. The method of light absorbed is identify of the composition. With control over sample thickness and depth the intensity of individual absorbing compounds can be used for this analysis. Every user provide reference of sample in positive substance 2 identification and compositional verification. FTIR can we use to identify chemical composition form paints polymers coating drugs and contaminates. The most powerful tool for identify FTIR is chemical bonding on functional group. The wavelength of light absorb is characteristic of the chemical bond. FTIR spectrometer was used to record in the meat IR region that is 400 to 4000 cm^{-1} .

4.3.4 Pair Distribution Function (PDF) –

Pair Distribution Function (PDF) is a technique that can provide structural information from disordered materials by using the powder XRD pattern. PDF analysis has been performed on the sample to calculate the bond distance and distance of atoms over short range region (local structure) and long range region (overall structure). The scattering function followed by the pair distribution function (PDF) was used to extract the structural information about the distribution of atoms. In this method, high energy X-Ray are scattered off nanomaterials and detector its much like in conventional powder diffraction experiment. The difference is the extreme short wavelength of X-rays that are used and wide range of angle measure over which they detected, as a result very wide range of reciprocal space to be probed. The real space refinement of crystal structure and the development of the capability to fit a theoretical three dimensional structure to atomic pair distribution function data from total scattering data which include both Bragg's peak and diffuse peak. In geometrical point of view the atomic PDF is a function gives the probability of finding atoms in a spherical shell

of unit thickness at a radial distance “ r ” from a reference atom. So the different peak position represents different bond length. Here we plot PDF [that is $G(r)$] with respect to radial distance “ r ” from an arbitrary origin and observed how the bond distance changes for different type of bond with addition of Zr and Ti.



Fig3.6: – Brukar D8 advance

4.3.5 Di-electric Measurement:-

The material electrical properties that will be mention here is permittivity and permeability. The information about resistivity and it's dimension, which can set by results for measuring permittivity and permeability with LRC measures. It is important that permeability and permittivity are not constant. They can change with apply temperature, pressure, frequency,

exposure, molecular structure and material quality. The term dielectric means immaterial can capable 2 store energy when and external electric field is applied. If a DC voltage source is applied on a parallel capacitor, to change is storage when dielectric material is between the plates then no materials in between the plates which is vacuum. The dielectric material to change storage capacity then neutralize the charge at the electrode. For increase storage capacity neutralize the charge. Which is contribute to the external field. The capacitance with the dielectric material is related to dielectric constant. If a DC voltage source is placed across a parallel plate capacitor more charges storage when a dielectric material is between the plates is no material. And dare the area of the capacitor plates and the thickness of plate. ϵ_0 = Permittivity of free space (8.854×10^{-12} F/m). The dielectric material increases the storage capacity of the capacitor by negative charges at the electrodes which naturally would contribute to the external field.

C=Capacitance (F)

a= area of plate (m^2)

D= Thickness of plate (m)

K= Dielectric constant

ϵ_0 = Permittivity of free space (8.854×10^{-12} F/m)

$$C = \frac{k\epsilon_0 A}{d}$$

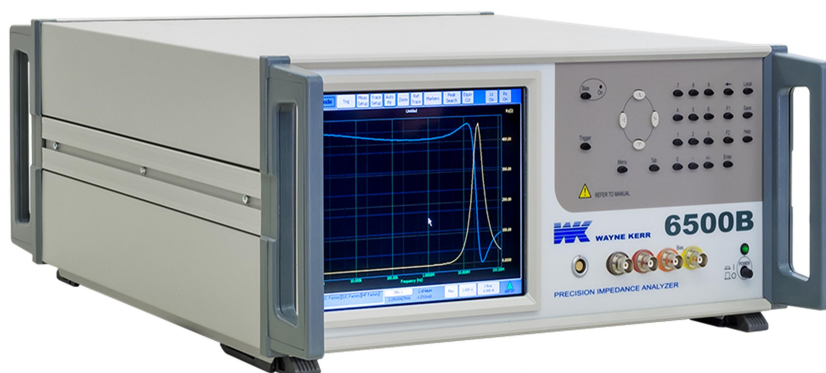


Fig.3.7:- Dielectric measurement instrument (Wayne kerr 6500B)

4.3.6 TGA and DTA –

TGA (Thermo-gravimetric analysis) determine mass loss over temperature. It's means when any sample heated then presented of water and calcinated sample evaluate into air, there for weight loss looking. And TGA differential thermal analysis, to determine endo and exothermic reaction in different temperature, also shows phase transition.

4.4 Experimental procedure:

BCZT ceramics were prepared via conventionally method by high energy ball milling. Commercial available powders of barium carbonate (BaCO_3) (99.98 % Sigma-aldrich), calcium carbonate (CaCO_3) (99.0% Sigma-aldrich), titanium dioxide (TiO_2) (99.98 % Sigma-aldrich) and zirconium oxide (ZrO_2) (99.9 % Sigma-aldrich), were used as starting materials with the nominal composition of **$\text{Ba}_{0.85}\text{Ca}_{0.15}\text{Zr}_{0.04}\text{Ti}_{0.96}\text{O}_3$** and **$\text{Ba}_{0.85}\text{Ca}_{0.15}\text{Zr}_{0.10}\text{Ti}_{0.90}\text{O}_3$** . The sample was doping via planetary ball milling (Fritsch ball milling) process. In this jar all sample has put into and rotate about 300 rpm for several hours and to get homogeneous mix zirconium ball are use. Several time after some sample are put out into the jar. During ball milling sample carried out for 10h, 50h, 70h, and 100 h. All four samples are send in Furness for calcination. The powder was calcined 1200 °C and 1 hours stand by, with constant increase rate 5°C/ min each sample. Calcinated powders were send in XRD division for finding geometry, and all sample analysed by FESEM, Thermogravimetric Analysis (TGA) Differential Thermal Analysis (DTA). DTA carried out from temperature at 20 to 1200 °C at constant rate of 10 °C/ min of heating in normal atmosphere in a DTG60 analyser. FTIR spectrometer was used to record the compositional bond in the mid IR spectrum (it's 400 to 4000 cm^{-1}). Calcinated powders use to determine dielectric constant making by pleats, two percentage of sample PVA was added into the powders as a binder and pressed into pellets at 20 Mpa by hand hydraulic pressed. The diameter was sintered sample is 10 mm and 2 mm thickness. All the pellets are coating with silver pest on both sides for better Conductance. The capacitance and resistance were measure by using Wayne Kerr 6500 Banalyser. For structure analyser of Calcinated powders performed by XRD (rigaku ultima). The X-Ray diffractometer operating at 40 kV and 40 ma with CuK ($\lambda = 1.5418 \text{ \AA}$) radiation, with the angle of 10 to 80 ,the steps size of measurement is 0.02 and counting time is 3 sec. XRD data was analysed by the Rietveld technique using Panalytical X'pert High Score Plus softeware. Micro structure and surface morphology

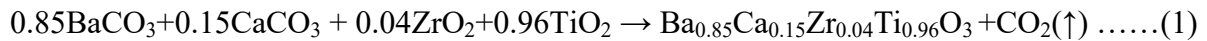
Chapter 5: Results and discussion

5.1 XRD analysis of BCZT powder-

5.1.1 Structural characterization for $\text{Ba}_{0.85}\text{Ca}_{0.15}\text{Zr}_{0.04}\text{Ti}_{0.96}\text{O}_3$ (BCZT-1)

XRD patterns Fig.5.1 of all the sample shows that BaTiO_3 contain Ca and Zr atom. Samples at different temperatures were taken to study the atomic position. BCZT (Tetragonal) phase having space group of $P4mm$ (space group number 99). BCZT (pseudo cubic) having space group $Pm-3m$ (space group number 221), and CaTiO_3 (cubic) space group $Pm-3m$ (space group number 221) [1].

XRD analysis has been conduct on the milling sample for study the structural change in the BT sample, at different meaning time. Figure one shows that XRD of milling BCZT sample transform phase have been reported by J. Ghosh [9]. The report at BT powders to change a continuous and diffusion dynamic phase transition involved. The phase transition from tetragonal (T) and pseudocubic (P) and cubic (C) phase appear. In this experiment total three series of sample analysis. In first series XRD pattern indicate tetragonal and pseudo cubic phase. In this experiment we see increase with milling time the sample change tetragonal to Monoclinic to pseudo cubic $[T > (T+M) > P]$ [2]. And for second series increase with milling time the sample transform tetragonal to Cubic. When ball milling BT powders heated for several hours in furnace at 1200 C, the BCZT nano-particle get convert in cubic phase with Cristal size 87 nm. In XRD pattern observe, with increase of milling time XRD peak become broader, it's indicate reduce particles size and increase lattice strain [6].



$\text{BaCO}_3=30.0$ gm, $\text{CaCO}_3= 2.69$ gm, $\text{ZrO}_2= 0.914$ gm, $\text{TiO}_2= 14.23$ gm Aldrich sample was taken for this series.

Table.5.1: Wt. % of phases, values of Unit cell parameters and Unit Cell volume as obtained by Rietvled Analysis for (BCZT-1).

| PARAMETER | | 10 hrs | 50 hrs | 70 hrs | 100 hrs |
|--------------------|---|-------------------------------------|-------------------------------------|-------------------------------------|-------------------------------------|
| Wt % Phases | | T=42.0% P=48.7% CT=9.3% | T=29.2% P=62.5% CT=8.3% | T=31.9% P=59.6% CT=8.5% | T=28.7% P=63.0% CT=8.4% |
| Cell parameter (Å) | T | a=3.99317 b=3.99317 c=4.01104 | a=3.98403 b=3.98403 c=4.00419 | a=3.98873 b=3.98873 c=4.00522 | a=3.9894 b=3.9894 c=4.00598 |
| | P | a=4.00892 b=4.00892 c=3.98799 | a=3.99145 b=3.99145 c=4.01171 | a=3.99212 b=3.99212 c=4.01329 | a=3.99294 b=3.99294 c=4.01376 |

| | | | | | |
|----------------------------------|----|---|--|--|--|
| | CT | a=5.44344 b=7.67817 c=5.40562 | a=5.44922 b=7.66929 c=5.41793 | a=5.44747 b=7.66825 c=5.41409 | a=5.44683 b=7.66755 c=5.41161 |
| Cell Volume (Å ³) | T | 63.95766 | 63.55654 | 63.72269 | 63.7565 |
| | P | 64.09282 | 63.91321 | 63.96007 | 63.9937 |
| | CT | 225.9314 | 226.4244 | 226.1603 | 226.0094 |
| Refinement details | | GOF =1.34318 R _e =13.55755 R _p =11.35961 R _{wp} =15.71259 | GOF =1.3949 R _e =12.69059 R _p =10.79082 R _{wp} =14.98877 | GOF =1.3225 R _e =12.54289 R _p =10.35664 R _{wp} =14.42458 | GOF =1.6723 R _e =9.32603 R _p =8.74919 R _{wp} =12.06042 |

T-Tetragonal, P- Pseudocubic, CT- Calcium titanate.

The Rietveld refinement method was used for crystal structure analysis. For quantitative phase analysis this technique is more precise over traditional single or multiple profile XRD Analysis[11]. All parameters can be simultaneously refined by least square method. The calculate pattern match with experimental data during Rietveld refinement [3]. In the present study we consider first order (110) reflection for the single profile analysis to calculate crystalline size and lattice strain of this sample. The crystal size and lattice strain was calculated with respect to (110) crystallographic plane which is known as Scherrer formula [8].

Crystallite size = $K\lambda / (B \cos \Theta)$, Lattice strain = $B / (4 \tan \Theta)$

where, B (size) = $B_{\text{obs}} - B_{\text{std}}$ & B (strain) = square root $(B_{\text{obs}}^2 - B_{\text{std}}^2)$.

in this equation, B referred as structure broadening, it is the difference between profile width, standard (B_{std}) and the experimental sample (B_{obs}). For single profile analysis standard CLAB6 was used [5,6]. Because the standard sample did not have any broadening or instrumental broadening in diffractometer. In table 2 shows crystalline size and lattice strain value.

Table.5.2: Value of crystalline size and lattice strain of Ba_{0.85}Ca_{0.15}Zr_{0.04}Ti_{0.96}O₃ (BCZT-1)

| Sample | BCZT 10hrs | BCZT 50hrs | BCZT 70hrs | BCZT 100hrs |
|-----------------------|------------|------------|------------|-------------|
| Crystallite size (nm) | 82.22 | 87.20 | 100.80 | 113.43 |
| Lattice Strain (%) | 0.0680 | 0.0163 | 0.0214 | 0.0296 |

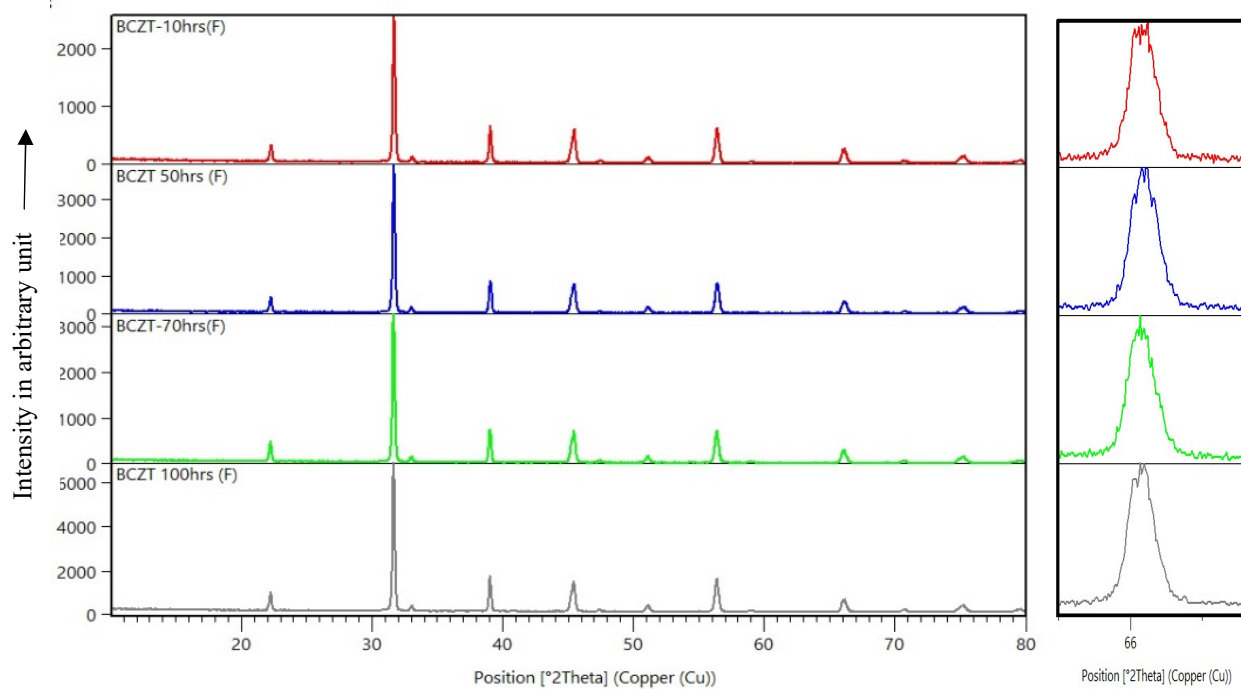


Fig.5.1:- XRD pattern of starting and milled (0-100 h) BCZT-1 sample

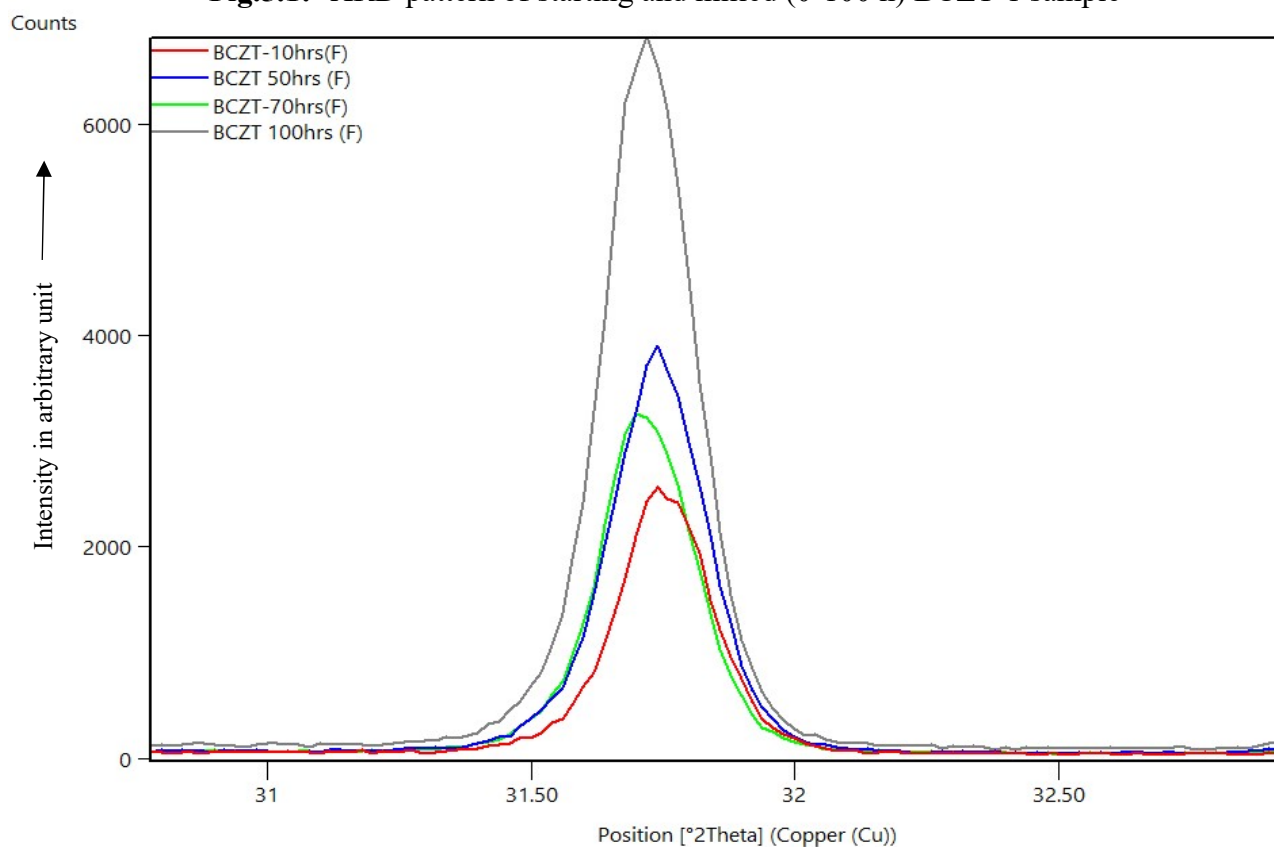
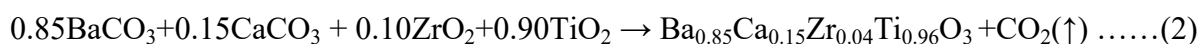


Fig.5.2:- Comparison of all XRD pattern at starting and milled (0-100 h) BCZT-1 sample

5.1.2 Structural characterization for Ba_{0.85}Ca_{0.15}Zr_{0.10}Ti_{0.90}O₃ (BCZT-2)

In this series percentage of Zr increase from 0.04 to 0.10 by conventional mixing by using ball milling and reduce particle size, under pressure ~6.5 Pa. calcination range 1200C with constant increase rate 5°C/min to achieve the maximum density.



BaCO₃=30.0 gm, CaCO₃= 2.69 gm, ZrO₂= 2.21gm, TiO₂= 12.89 gm Aldrich sample was taken for this series.

Table.5.3: Wt. % of phases, values of Unit cell parameters and Unit Cell volume as obtained by Rietveld Analysis in BCZT-2.

| PARAMETER | 10 hrs | | 50 hrs | 70 hrs | 100 hrs |
|-------------------------------|---|-------------------------------------|---|--|--|
| Wt % Phases | T=47.2% C=49.1% CT=3.7% | | T=65.9% C=29.3% CT=4.8% | T=49.5% C=48.9% CT=1.6% | T=58.2% C=39.1% CT=2.7% |
| Cell parameter (Å) | T | a=4.01208 b=4.01208 c=4.02042 | a=4.01196 b=4.01196 c=4.01868 | a=4.01036 b=4.01036 c=4.01638 | a=4.01029 b=4.01029 c=4.01688 |
| | C | a=4.01151 b=4.01151 c=4.01151 | a=4.01966 b=4.01966 c=4.01966 | a=4.01768 b=4.01768 c=4.01768 | a=4.01862 b=4.01862 c=4.01862 |
| | CT | a=3.83 b=3.83 c=3.83 | a=3.83 b=3.83 c=3.83 | a=3.83 b=3.83 c=3.83 | a=3.83 b=3.83 c=3.83 |
| Cell Volume (Å ³) | T | 64.71565 | 64.68383 | 64.59546 | 64.60124 |
| | C | 64.55404 | 64.94819 | 64.85234 | 64.89816 |
| | CT | 56.18189 | 56.18189 | 56.18189 | 56.18189 |
| Refinement details | GOF =1.57501 R _e =13.98717 R _p =13.666 R _{wp} =17.55379 | | GOF =1.1354 R _e =12.51772 R _p =10.64592 R _{wp} =13.3381 | GOF =1.1884 R _e =12.63968 R _p =11.21145 R _{wp} =13.77896 | GOF =1.1147 R _e =14.1081 R _p =12.12569 R _{wp} =14.8958 |

T-Tetragonal, C- Cubic, CT- Calcium titanate.

Wt.% of phases, the values of cell parameters and cell volume, of these phase were estimated for this sample form X-ray diffraction (XRD) line profile analysis using Rietveld analysis by X'pert high score plus software (PAN alytical) and the values are shown in the Table.5.3. The quality of fitting was also assessed from various numerical criteria of fit, namely the profile residual factor (R_p), the expected residual factor (R_{exp}) the weighted R profile (R_{wp}) and the goodness of fit (GOF), as obtained from Rietveld analysis, all relating good fitting and values are shown in Table.5.3 The quality of the fittings of observed diffraction patterns with the simulated patterns are shown by difference plots in Fig.5.3

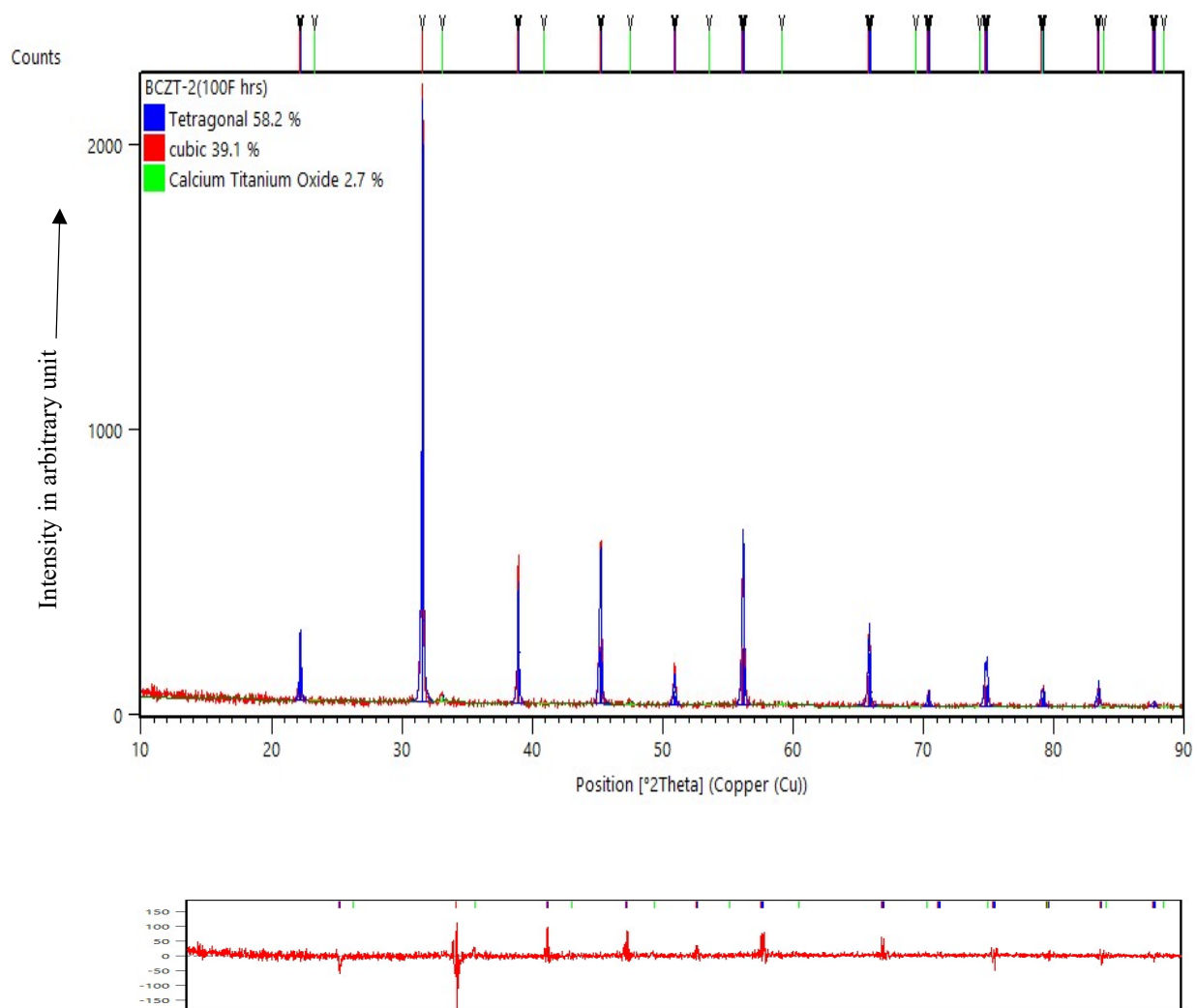


Fig.5.3:- Rietveld refinement of BCZT-2 (100 hrs)

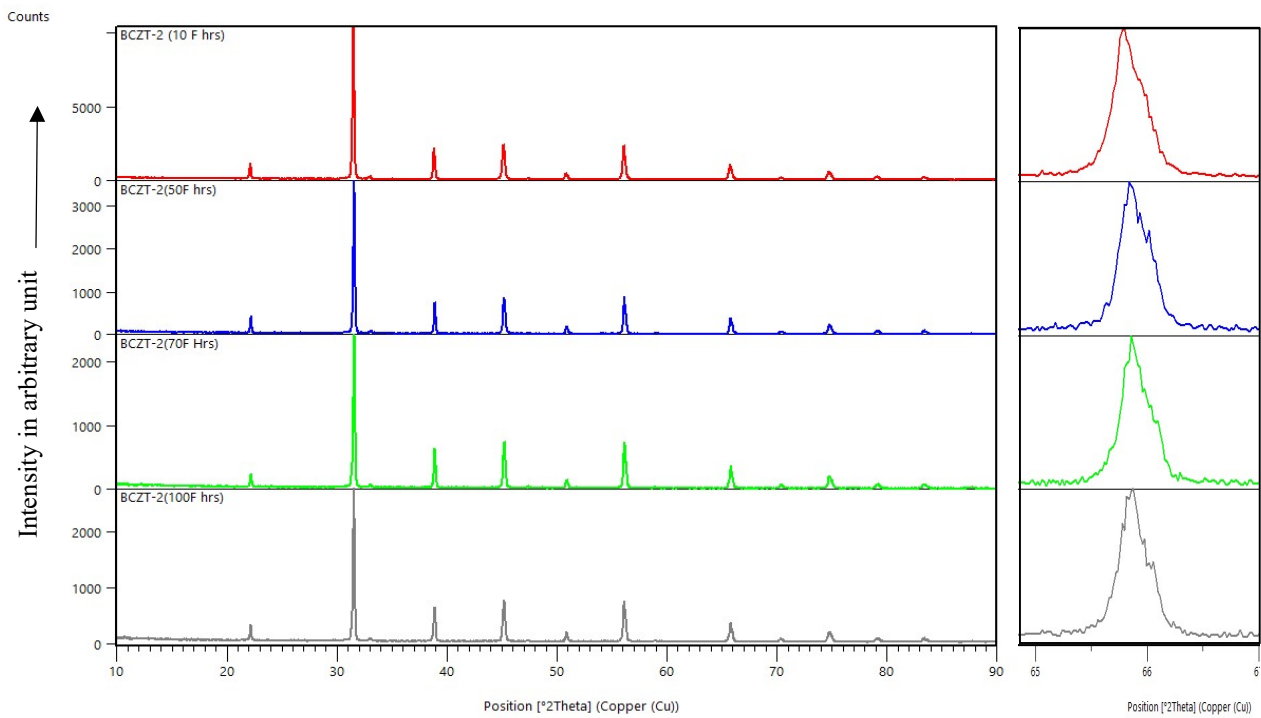


Fig.5.4:- XRD pattern of starting and milled (0-100 h) BCZT-2 sample

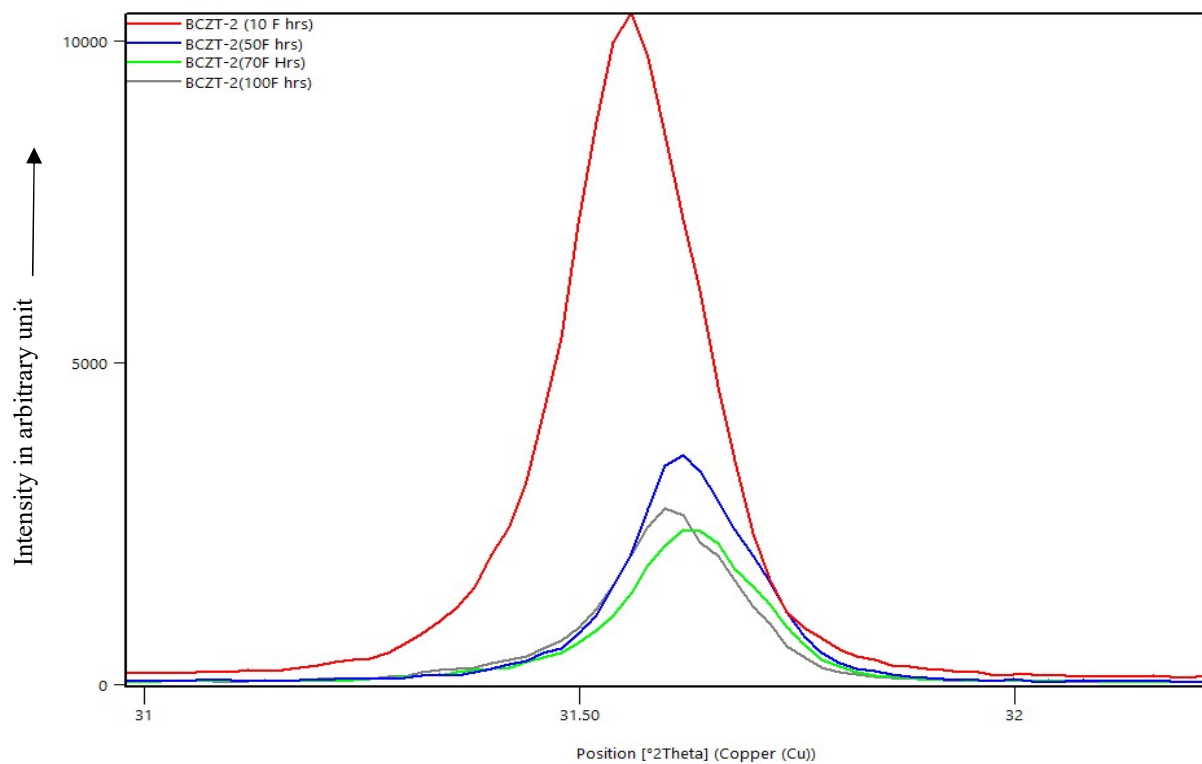


Fig.5.5:- Comparison of all XRD pattern at starting and milled (0-100 h) BCZT-2 sample

Table.5.4: Value of crystalline size and lattice strain of $\text{Ba}_{0.85}\text{Ca}_{0.15}\text{Zr}_{0.10}\text{Ti}_{0.90}\text{O}_3$

| Sample | Peak position(2θ) | B_{obs} | B_{std} | Crystallite size(nm) | Lattice Strain(%) |
|-------------|----------------------------|------------------|------------------|----------------------|-------------------|
| BCZT 10 hrs | 31.5595 | 0.1771 | 0.0934 | 98.3 | 0.233 |
| BCZT 10 hrs | 31.6228 | 0.1605 | 0.0934 | 121.4 | 0.202 |
| BCZT 10 hrs | 31.6294 | 0.1714 | 0.0934 | 105.9 | 0.221 |
| BCZT 10 hrs | 31.6077 | 0.1652 | 0.0934 | 114.7 | 0.210 |

5.2 PDF analysis-

Experimental PDF is shown in figure.5.6. Intensity of the PDF peaks changes with distance of atom and bond with atoms. Different bond distance of the BT nano-crystalline sample obtained from PDF [24]. First pair of Ti-O situated around 2.06 Å. Then the next two peaks at 2.87 Å and 3.419 Å were Ba-O and Ba-Ti first distances [23]. The slight differences in the PDF value of Ba-O and Ba-Ti distance were change with Rietveld value [25] due to local structure distortion, due to off-centring of Ti atoms in BaTiO_3 .

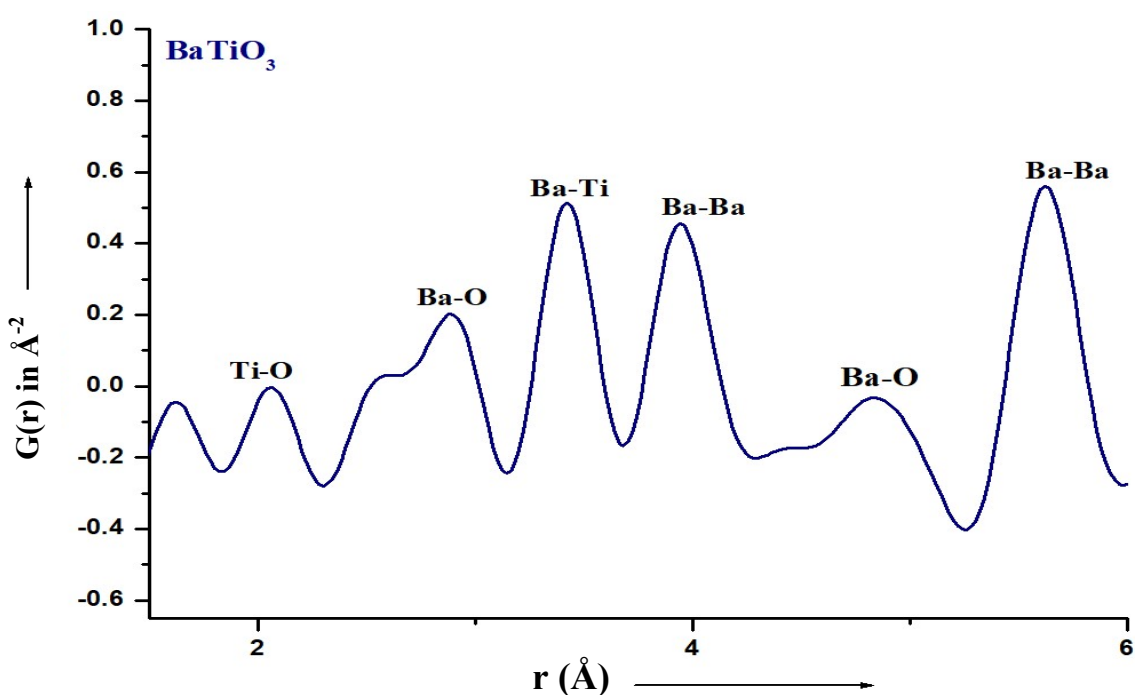


Fig.5.6:- Different bond distance and atomic arrangements of BaTiO_3 obtained from PDF

Table.5.5:- comparison of different bond distance and atomic arrangements of BaTiO₃ obtained from PDF

| Bond present in Pure BaTiO₃ | Atomic Pair distance (Å) | |
|---|---|---|
| | Pair Distribution Function (PDF) | As obtained by Rietveld analysis |
| Second Ti-O | 2.0599 | 2.03 |
| Second Ba-O | 2.8799 | 2.869 |
| First Ba-Ti | 3.4199 | 3.51 |
| First Ba-Ba | 3.9399 | 4.00 |
| Fourth Ba-O | 4.8400 | 4.374 |
| Third Ba-Ba | 5.6190 | 5.657 |

5.3 FESEM analysis; -

The Grain size and surface morphology and different magnification was analysis by the field emission electron microscope (FESEM). In FESEM observed the BCZT particles are agglomerate and cubic shape with homogenous grain [fig.5.7.1 to 5.7.6]. Due to high impact on the powder sample nano particle get agglomerate to each other. The pure BT consists of spherical and plate like shape. The addition of Ca and Zr to decrease the grain size and increase density[15]. Heated BCZT contains spherical and cubic like shape. The distribution of Ca and Zr into BT was further confirmed by EDX [17]. Here we clearly see that particle size reduces from 80 nm to 30 nm. The average particle size of 10 hrs BCZT-1 was 56.26 nm and 100 hrs BCZT-2 was 45.10 nm measures from FESEM image[fig.5.8]. Since from FESEM image observed that some tiny particles are attached on the surface of grains.

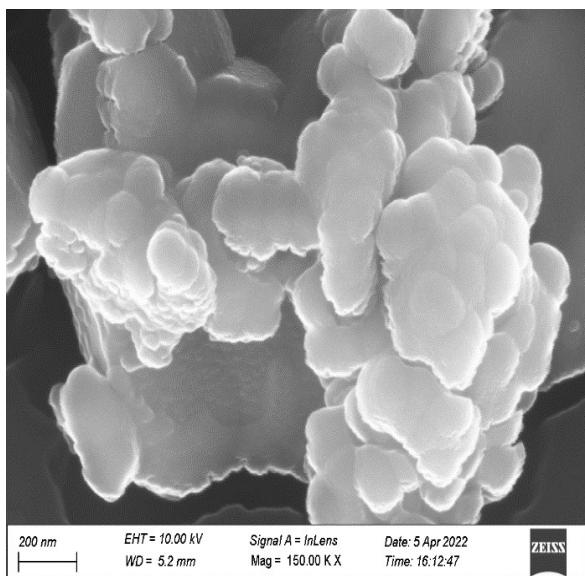


Fig.5.7.1-FESEM image of BCZT-1 (10 hr).

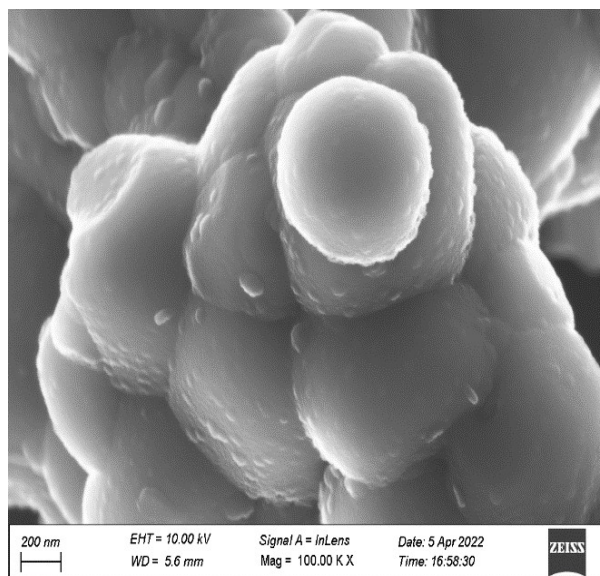


Fig.5.7.2-FESEM image of BCZT-1 (50 hr)

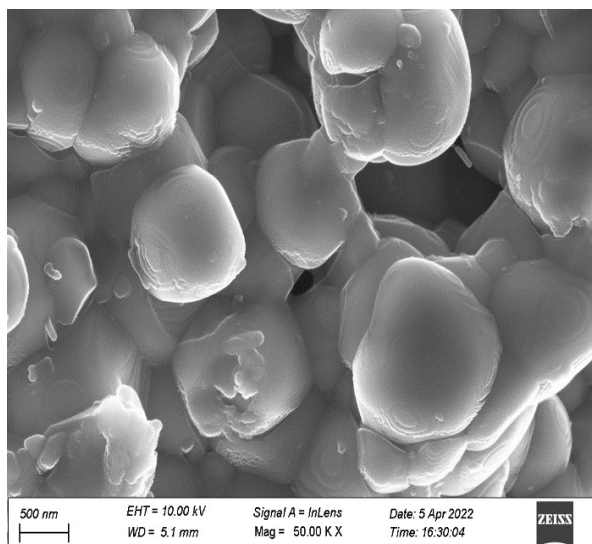


Fig.5.7.3-FESEM image of BCZT-1 (100 hr)

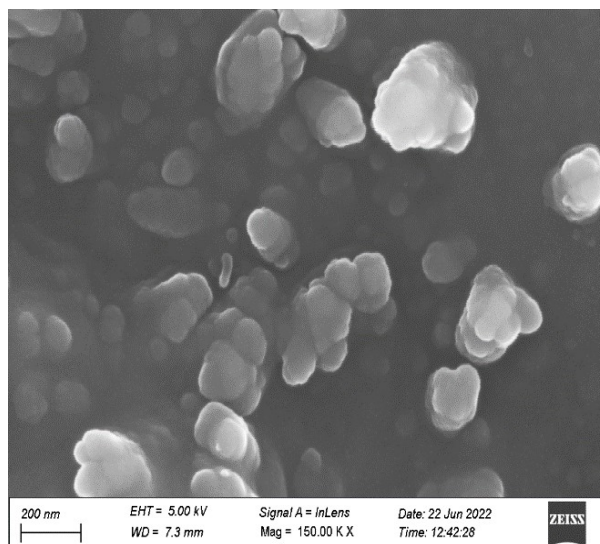


Fig.5.7.4 -FESEM image of BCZT-2 (10 hr)

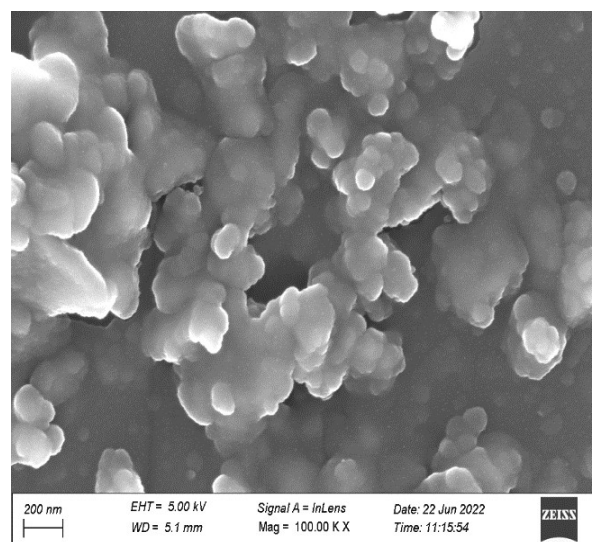


Fig.5.7.5-FESEM image of BCZT-2 (50 hr)

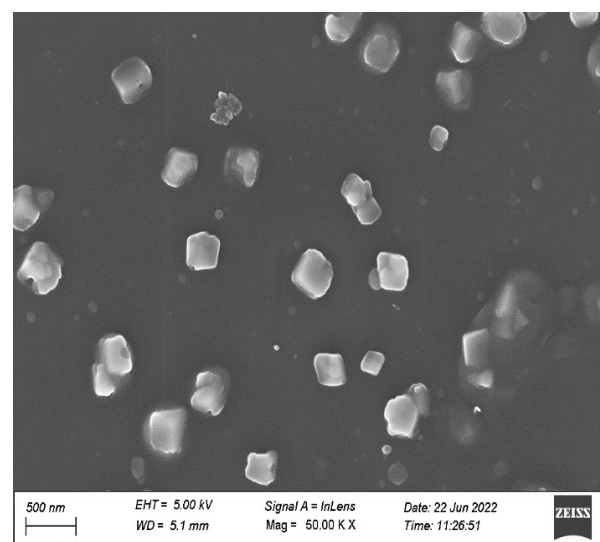


Fig.5.7.6-FESEM image of BCZT-2 (100 hr)

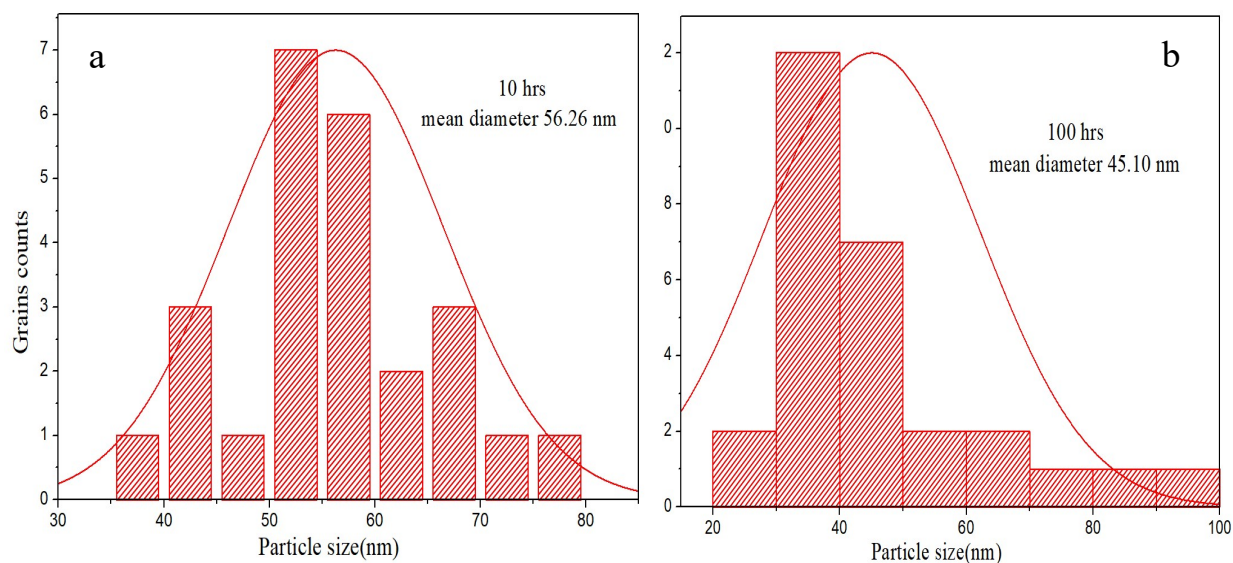


Fig 5.8: Particle size variation with milling hrs (a) BCZT-1 and (b) BCZT-2 obtain from FESEM

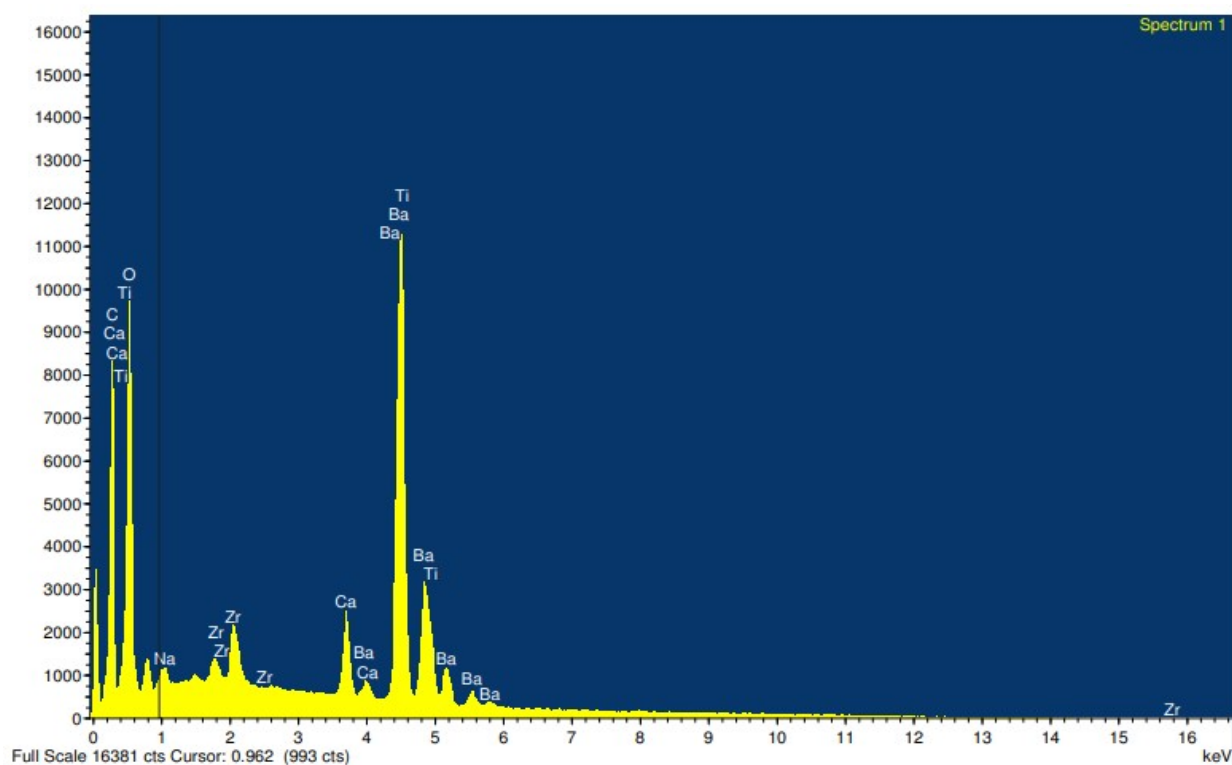


Fig.5.9: EDX spectra BCZT ceramic sample

5.4 FTIR (Fourier Transform Infrared Spectroscopy) –

FTIR confirmed that the BCZT formation of monophonic nature. FTIR spectra conform for the metallic bond between the atoms. The powders were prepared by head treatment at various temperature. The functional groups can be identifying by the infrared radiation. The functional group region (FGR) from wave number ($3500\text{--}1500\text{ cm}^{-1}$) and the Finger Print Region (FPR) having wave number $1500\text{--}400\text{ cm}^{-1}$ fig.5.10. Small shift was observed by adding of Zr and Ca doped in 50 hrs milling sample [21]. The absorption bands are observed in $500\text{ to }700\text{ cm}^{-1}$ range. In this range mainly metal oxide bond formation (Ba-O, Ca-O, Zr-O and Ti-O) [19,20]. The peak shifting is clearly indicate the melting point[fig.5.10], and peak decrease due to impurity present in the sample.

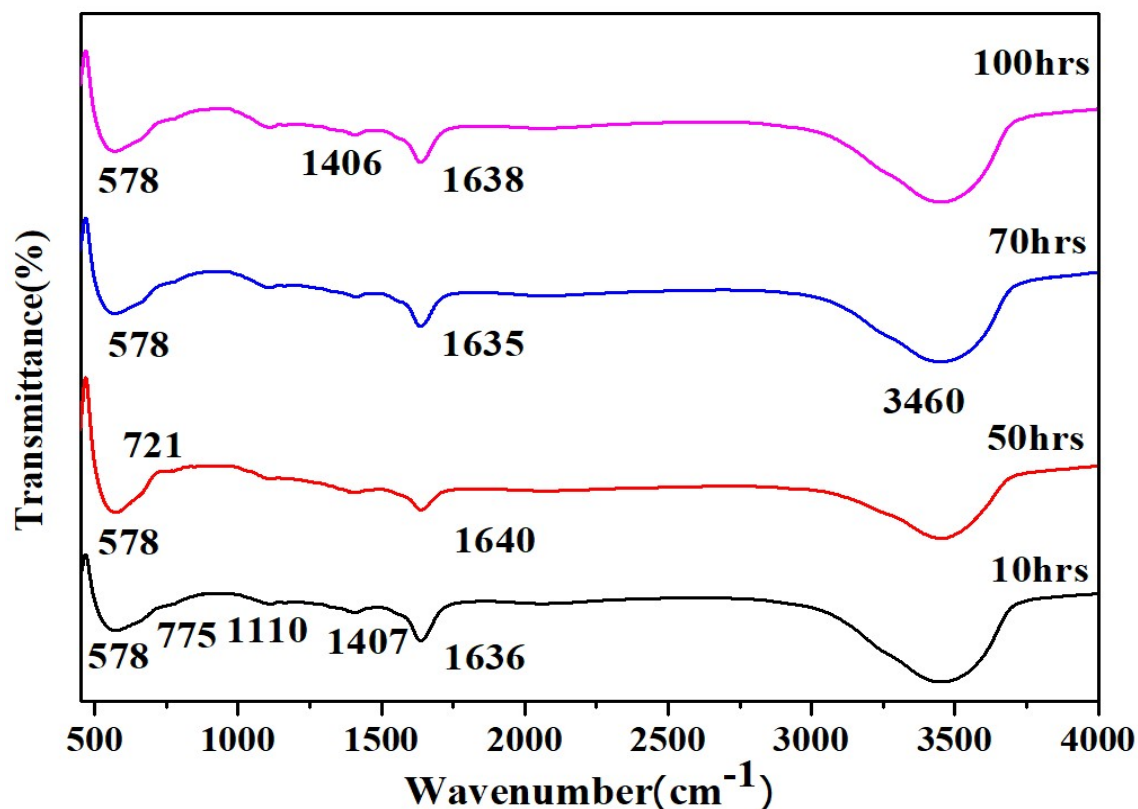


Fig.5.10:- FTIR spectra of heat treated powder at different ball milling time.

A strong bond peak observed at 3460 cm^{-1} is asymmetric and symmetrical OH stretching due to water absorption on the sample [22].

5.5 TGA _ DTA Analysis-

The total weight loss observed from TGA is around 18.45%. At $84\text{ }^{\circ}\text{C}$ first endothermic reactions take place. In the temperature range of $35\text{ to }350\text{ }^{\circ}\text{C}$ the hydration of water reflects, at $84\text{ }^{\circ}\text{C}$ carbon monoxide release from the precursor which reflect small peak at 544°C

[15,16]. In temperature range 20 to 500 C the weight loss is 1.99%. The second step is thermal decompose of oxide in temperature range 500 to 775 C, in this range Endo ii (544C) and Endo iii (709) observed [17], and as a results carbon monoxide and carbon dioxide release. The experimentally observed the weight loss in temperature range is 3.42% of total weight of sample fig.5.11. The residue present in this range is $\text{Ba}_{0.85}\text{Ca}_{0.15}\text{Zr}_{0.1}\text{Ti}_{0.9}\text{O}_3 + \text{CO}_3$. The final decomposition occurred in 775 to 900C range. In this range Endo iv(824C) and Endo v (879 C) observed [18], and carbon dioxide release in this range. And final results is $\text{Ba}_{0.85}\text{Ca}_{0.15}\text{Zr}_{0.04}\text{Ti}_{0.96}\text{O}_3$. In final stage weight loss is 13.04%.

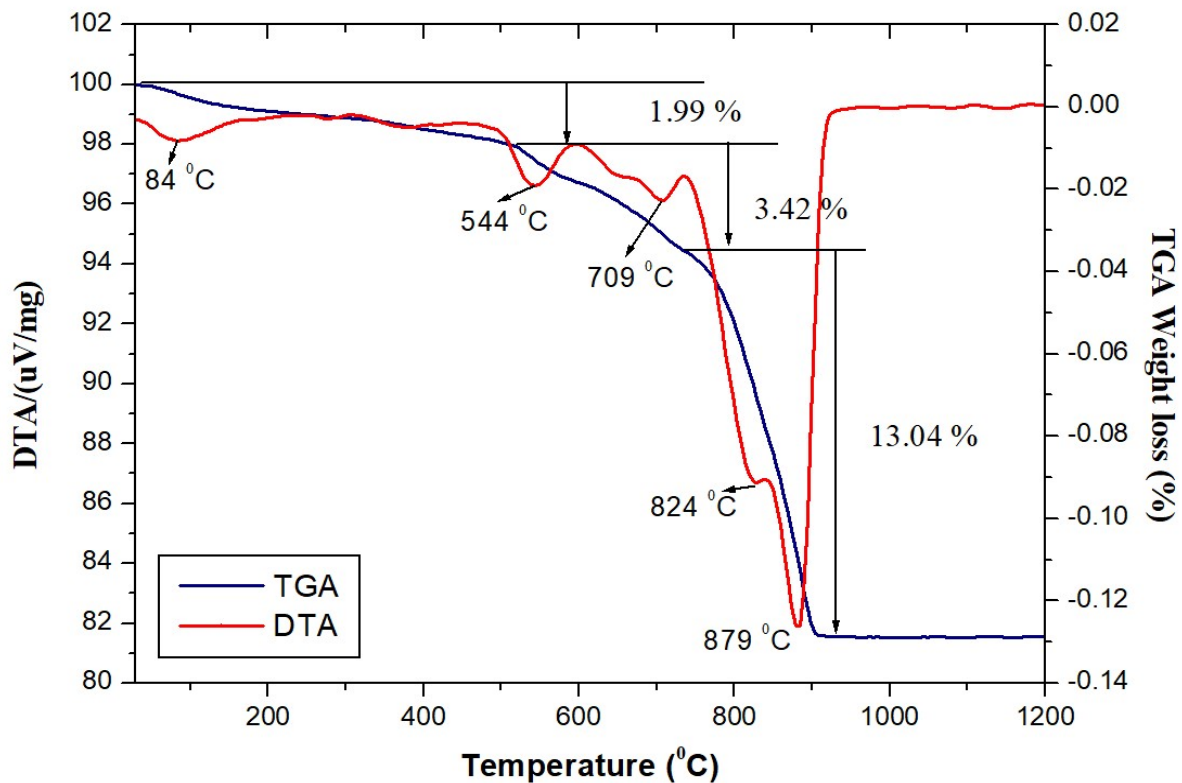


Fig.5.11:- DTA-TGA curves obtain from BCZT powder

5.6 Dielectric constant

Fig.5.12. Show that The sintered BCZT dielectric constant depends on temperature also variations of frequency. The dielectric value of all ceramic sample summarized in table. All sample shows a dielectric range associated with tetragonal to cubic phase transition. The unique dielectric value notice in the temperature range 50 hrs. All peak depends on temperature and frequency with higher temperature shift with increasing frequency. The phenomena can be explained by the graph of frequency with capacitance and resistance [12,13]. The dielectric value decrease with increase cubic phase president in sample. So increase ball milling time with increase temperature the crystal transfer to tetragonal to cubic that's why dielectric value decrease, because cubic structure is centro-symmetric nature there for net polarization decrease[19].

Table.5.6: Dielectric and capacitance in different milling time variation

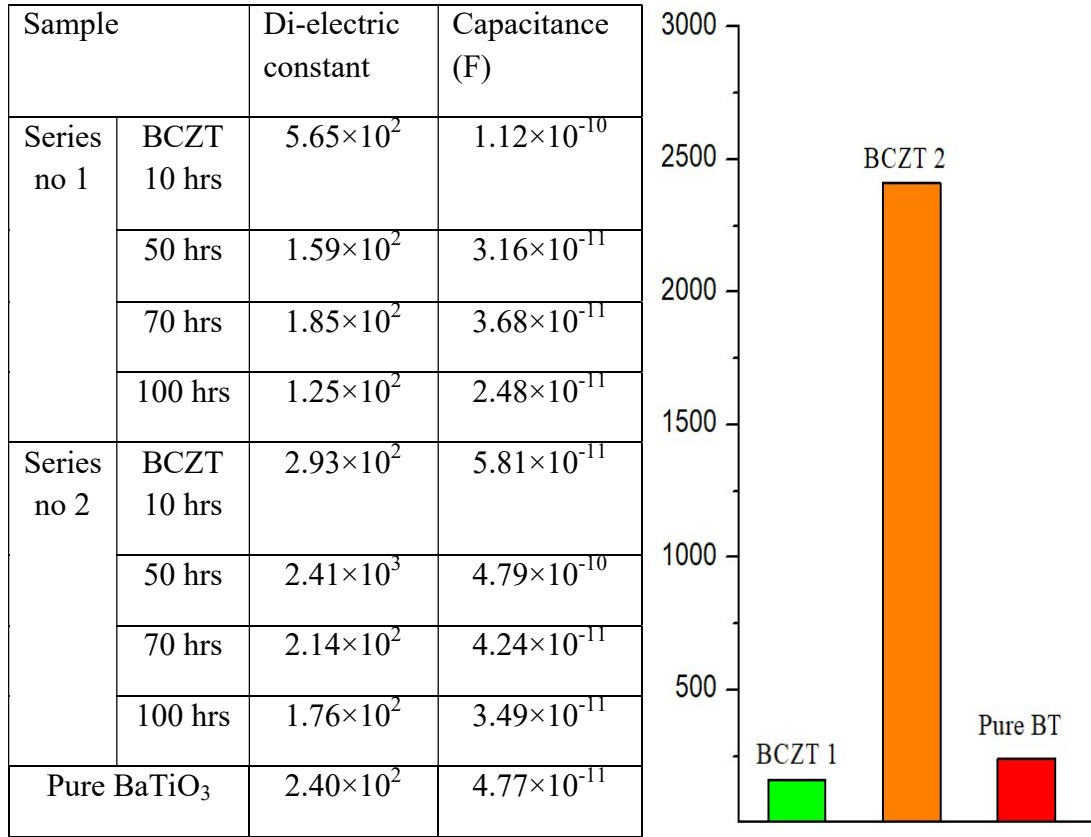


Fig.5.12: Dielectric value of BCZT-1, BCZT-2 and Pure BT sample

Chapter 6: Conclusion and Future Scope

6.1. Conclusion

In this study, lead free $\text{Ba}_{0.85}\text{Ca}_{0.15}\text{Zr}_{0.04}\text{Ti}_{0.96}\text{O}_3$ (BCZT-1) and $\text{Ba}_{0.85}\text{Ca}_{0.15}\text{Zr}_{0.10}\text{Ti}_{0.90}\text{O}_3$ (BCZT-2) and pure BaTiO_3 (BT) ceramics have been successfully prepared by High energy ball milling process. The average crystallographic structure was determine by XRD, here tetragonal BT transform to pseudocubic with increase ball milling time, and local atomic scale structure was determine by PDF. Particle size reduces from 80 nm to 40 nm with increase ball milling time. Metallic bond (Ti-O, Ba-O, Ba-Ti, Ba-Ba) reported from PDF curve fitting, which is also compare with Rietveld analysis. Two distinct peaks in PDF of 100 h milled BT appeared at $r=3.419 \text{ \AA}$ and $r=3.939 \text{ \AA}$ which was due to higher intensity of Ba-Ti and Ba-Ba pair. The short range tetragonal and long range cubic structure reported from PDF curve fitting. Highest dielectric value reported in 50 hrs ball-milled sample, because higher percentage of tetragonal phase and lower percentage of cubic phase present as reported from Rietveld analysis.

For BCZT-1 series, dielectric constant decrease with respect to BT and BCZT-2. For 0.04 Zr doped cell structure of BCZT convert into higher percentage of pseudocubic phase. Presence of moisture and carbon (C) in atmosphere some amount of BCZT convert into the Calcium titanate (CaTiO_3). Due to high in temperature heating and small amount of Zr doped off-centring Ti move to centre. It was observed from Rietveld analysis BCZT transform into pseudocubic phase with 63 percentages. Spherical structure retort from FESEM, and size reduction from 80 nm to 56.26 nm.

For BCZT -2 series, dielectric response high due to higher percentage of off-centring tetragonal phase appear in XRD. With increasing Zr doped phase formation of CT and cubic phase decrease. With increase of Zr, the dielectric constant maximum [fig.5.11] value increase first 50 hrs and with further increase milling hrs dielectric value decrease such phenomena indicate phase transition. In Rietveld, it was clearly observed cubic phase decrease with increase milling time. The lowest cubic phase observed in 50 hrs milled sample. Therefore highest dielectric response shows in 50 hrs milled sample is 2.41×10^3 . During ball milling process with increase in time BCZT-2 ceramic with decrease particle size from 80 nm to 45.10 nm. In FTIR analysis we observed metallic bond present in between 500 to 700 cm^{-1} range. And total weight loss in calcination process is 18.45% wt. of sample observed in TGA analysis. XRD, PDF and FESEM revealed that BCZT ceramics transform pure perovskite phase with tetragonal to pseudocubic to cubic phase. Using FESEM we get information about surface morphology, micro structure, geometry and particle size. In BCZT ceramic with increase Zr concentration dielectric response also increase.

6.2. Future Scopes:

- The present work focused on local structure investigation of BCZT ceramics using X-Ray Diffraction (XRD) and Pair Distribution Function (PDF) technique. Atomic scale structure of BT has been explored using PDF. Atomic scale structure of BT after adding dopant (Ca, Zr, Sr etc.) will be explore in my future work.
- Since BaTiO₃ nano materials have great application in MLCC, some other dopant (like Nb 5+, Mn, Al, Fe etc) can be use and study the effect of distribution of these dopants on overall performance of nano-structured perovskite for the development of super capacitance.
- In future attempts, this material could use to the developed capacitance, which is use in chip industry.

6.3. Publications:

1. “Synthesis of Ca, Zr co-doped nano-structured BaTiO₃ by high energy ball milling” authored by Amit Maity, Santanu Sen and Jiten Ghosh, **Glamics Fiesta-2022, organized by Central Glass and Ceramics Research Institute.**
2. “Local structural investigation of Zr & Ca doped BaTiO₃ nanocrystals” ; this paper will be communicate in SCI Journal.

Reference:

- [1]. Tian, Yongshang, et al. "Low-temperature sintering and electric properties of BCT–BZT and BCZT lead-free ceramics." *Journal of Materials Science: Materials in Electronics* 26.6 (2015): 3750-3756.
- [2]. Hanani, Zouhair, et al. "Enhanced dielectric and electrocaloric properties in lead-free rod-like BCZT ceramics." *Journal of Advanced Ceramics* 9.2 (2020): 210-219.
- [3]. Abhinay, S., P. Tarai, and R. Mazumder. "Preparation and characterization of (Ba_{0.85}Ca_{0.15})(Zr_{0.1}Ti_{0.9}) TiO₃ (BCZT)/Bi₂O₃ composites as efficient visible-light-responsive photocatalysts." *Journal of Materials Science* 55.5 (2020): 1904-1914.
- [4]. Verma, Ritesh, et al. "Structural, optical, and electrical properties of vanadium-doped, lead-free BCZT ceramics." *Journal of Alloys and Compounds* 869 (2021): 159520.
- [5]. Ji, Xiang, et al. "Structural and electrical properties of BCZT ceramics synthesized by sol–gel-hydrothermal process at low temperature." *Journal of Materials Science: Materials in Electronics* 30.13 (2019): 12197-12203.
- [6]. Buatip, N., et al. "Investigation on electrical properties of BCZT ferroelectric ceramics prepared at various sintering conditions." *Integrated Ferroelectrics* 187.1 (2018): 45-52.
- [7]. Hanani, Zouhair, et al. "Structural, dielectric, and ferroelectric properties of lead-free BCZT ceramics elaborated by low-temperature hydrothermal processing." *Journal of Materials Science: Materials in Electronics* 31.13 (2020): 10096-10104.
- [8]. Hanani, Zouhair, et al. "Morphogenesis mechanisms in the hydrothermal growth of lead-free BCZT nanostructured multipods." *CrystEngComm* 23.30 (2021): 5249-5256.
- [8]. Barman, Abhisikta, et al. "Large electrocaloric effect in lead-free ferroelectric Ba_{0.85}Ca_{0.15}Ti_{0.9}Zr_{0.1}O₃ thin film heterostructure." *APL Materials* 9.2 (2021): 021115.
- [9]. Shi, Min, et al. "Effect of annealing processes on the structural and electrical properties of the lead-free thin films of (Ba_{0.9}Ca_{0.1})(Ti_{0.9}Zr_{0.1}) O₃." *Journal of alloys and compounds* 562 (2013): 116-122.
- [10]. Luo, Bingcheng, et al. "Fabrication, characterization, properties and theoretical analysis of ceramic/PVDF composite flexible films with high dielectric constant and low dielectric loss." *Journal of Materials Chemistry A* 2.2 (2014): 510-519.

- [11]. Hanani, Zouhair, et al. "Enhancement of dielectric properties of lead-free BCZT ferroelectric ceramics by grain size engineering." *Superlattices and Microstructures* 127 (2019): 109-117.
- [12]. Liu, X., et al. "Ferroelectric, dielectric and pyroelectric properties of Sr and Sn codoped BCZT lead free ceramics." *Advances in Applied Ceramics* 114.8 (2015): 436-441.
- [13]. Abhinay, S., P. Tarai, and R. Mazumder. "Preparation and characterization of (Ba_{0.85}Ca_{0.15})(Zr_{0.1}Ti_{0.9}) TiO₃ (BCZT)/Bi₂O₃ composites as efficient visible-light-responsive photocatalysts." *Journal of Materials Science* 55.5 (2020): 1904-1914.
- [14]. Dixit, Pragya. *Fabrication and Characterization of PVDF-Ba_{0.8}Ca_{0.15}Zr_{0.1}Ti_{0.9}O₃ (BCZT) Composite Films*, Diss. 2018.
- [15]. Frattini, A., et al. "BCZT ceramics prepared from activated powders." *Procedia Materials Science* 1 (2012): 359-365.
- [16]. Castkova, Klara, et al. "Chemical synthesis, sintering and piezoelectric properties of Ba_{0.85}Ca_{0.15}Zr_{0.1}Ti_{0.9}O₃ lead-free ceramics." *Journal of the American Ceramic Society* 98.8 (2015): 2373-2380.
- [17]. Hikmah, Nahariatul, and Suasmoro Suasmoro. "Sintesis (Ba_{0.5}Ca_{0.5})(Zr_{0.5}Ti_{0.5}) O₃ dengan Metode Reaksi Padat." *Jurnal Sains dan Seni ITS* 3.2 (2014): B27-B29.
- [18]. Manohar, Chelli Sai, et al. "Novel lead-free biocompatible piezoelectric hydroxyapatite (HA)–BCZT (Ba_{0.85}Ca_{0.15}Zr_{0.1}Ti_{0.9}O₃) nanocrystal composites for bone regeneration." *Nanotechnology Reviews* 8.1 (2019): 61-78.
- [19]. Ji, Xiang, et al. "Structural and electrical properties of BCZT ceramics synthesized by sol–gel-hydrothermal process at low temperature." *Journal of Materials Science: Materials in Electronics* 30.13 (2019): 12197-12203.
- [20]. Ji, Xiang, et al. "Structure and electrical properties of BCZT ceramics derived from microwave-assisted sol–gel-hydrothermal synthesized powders." *Scientific Reports* 10.1 (2020): 1-8.
- [21]. Lu, Haowei, et al. "Polarization and space charge performance in PVDF with MPB composition BCZT doped composite films." *Journal of Applied Polymer Science* 134.40 (2017): 45362.
- [22]. Lu, Haowei, et al. "Improved dielectric strength and loss tangent by interface modification in PI@ BCZT/PVDF nano-composite films with high permittivity." *Journal of Materials Science: Materials in Electronics* 28.18 (2017): 13360-13370.

- [23]. Takada, Eri, et al. "Piezoelectric Properties and Local Structure Analysis of $(1-x)(\text{Na}_{0.50}\text{K}_{0.45}\text{Li}_{0.05})\text{NbO}_{3-x}(\text{Ba}_{0.85}\text{Ca}_{0.15})(\text{Zr}_{0.10}\text{Ti}_{0.90})\text{O}_3$ Solid Solutions Produced by Malic Acid Complex Solution Method." *Transactions of the Materials Research Society of Japan* 42.2 (2017): 27-30.
- [24]. Culbertson, Charles McLouth, et al. "The local structure of $0.5 \text{Ba}(\text{Zr}_{0.2}\text{Ti}_{0.8})\text{O}_3-0.5(\text{Ba}_{0.7}\text{Ca}_{0.3})\text{TiO}_3$ from neutron total scattering measurements and multi-edge X-ray absorption analysis." *Materials Research Bulletin* 135 (2021): 111124.
- [25]. Pan, Zhongbin, et al. "Ultrafast discharge and enhanced energy density of polymer nanocomposites loaded with $0.5(\text{Ba}_{0.7}\text{Ca}_{0.3})\text{TiO}_3-0.5 \text{Ba}(\text{Zr}_{0.2}\text{Ti}_{0.8})\text{O}_3$ one-dimensional nanofibers." *ACS applied materials & interfaces* 9.16 (2017): 14337-14346.
- [26]. Hanani, Zouhair, et al. "Enhancement of dielectric properties of lead-free BCZT ferroelectric ceramics by grain size engineering." *Superlattices and Microstructures* 127 (2019): 109-117.
- [27] P. Kumar, C. Prakash, O.P. Thakur, R. Chatterjee, T.C. Goel, Dielectric, ferroelectric and pyroelectric properties of PMnT ceramics, *Phys. B Condens. Matter.* 371 (2006) 313–316. doi:10.1016/j.physb.2005.10.107.

Thank You

“Nothing is impossible to the willing heart”

-Thomas Heywood